

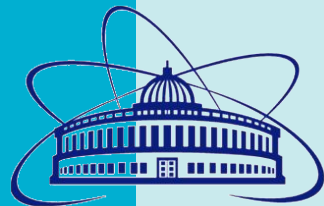


Seminario de Física de Altas Energías, ICN UNAM

Status of the MPD experiment at NICA.

Ivonne Maldonado

October 30th, 2024



Outline

1. Introduction
2. NICA complex
3. MPD experiment
4. MBB sub-detector
5. MPD physics program
6. Participation of Mexican Group
7. Summary

Heavy Ion Collisions (HIC)

- ★ QCD is a fundamental theory of the strong interactions
- ★ Only colorless particles are observed in the experiment \Rightarrow Confinement
- ★ QGP is a state of matter in which quarks and gluons are free to move in space \Rightarrow size of the nucleon

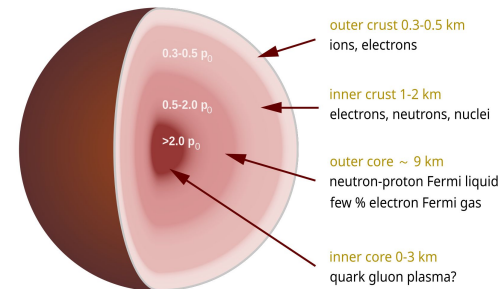
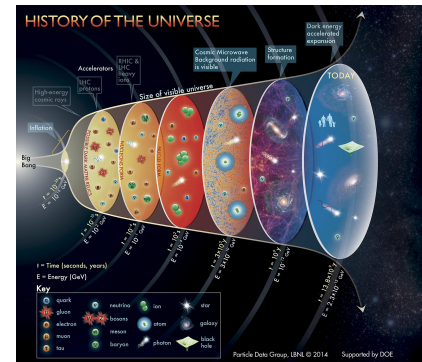
Two recipes for QGP Formation:

- ★ at high T , $\mu_B \approx 0 \Rightarrow$ Early Universe

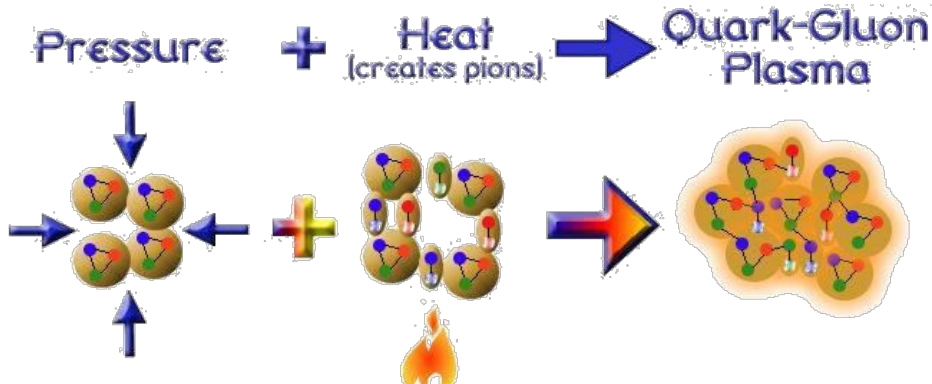
$$\sqrt{s_{NN}} > 100 \text{ GeV}$$

- ★ at intermediate T , high baryon density μ_B – Inner structure of the compact stars and neutron STARS mergers

$$2.4 \text{ GeV} < \sqrt{s_{NN}} < 11 \text{ GeV}$$



Relativistic heavy Ion collisions – a combination of the two recipes

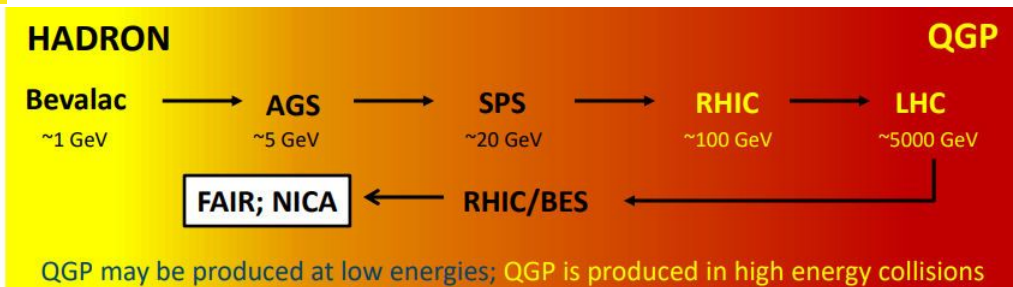


Short Heavy Ion-physics history

- **BEVALAC- LBNL** 1972 -1984 max. $\sqrt{s_{NN}} = 2.2 \text{ GeV}$
- **SPS - CERN** 1986 -2000 $\sqrt{s_{NN}} = 17.3 \text{ GeV}$
- **AGS - BNL** 1988 -1996 $\sqrt{s_{NN}} = 4.8 \text{ GeV}$
- **SIS 18 - GSI** 1990 $\gg \sqrt{s_{NN}} = 2.4 \text{ GeV}$
- **RHIC -BNL** 2000-2025 $\sqrt{s_{NN}} = 200 \text{ GeV}$
- **LHC - CERN** 2010 $\gg \sqrt{s_{NN}} = 5.02 \text{ TeV}$

Near Future

- FXT & Coll NICA -JINR 2024 $\sqrt{s_{NN}} = 11 \text{ GeV}$
- FXT SIS 100 - FAIR 2028? $\sqrt{s_{NN}} = 5 \text{ GeV}$



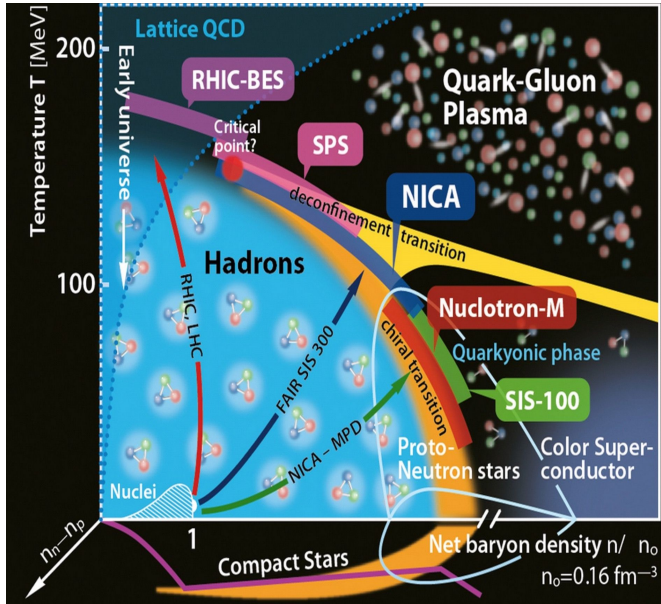
1970-2000 – nuclear equation of state (EoS), search for the quark-gluon plasma (QGP)

2005 – QGP formation was observed at RHIC and it behaves as almost perfect liquid

2005-2010 – LQCD predicts crossover phase transition at top RHIC and LHC (high T , $\mu \approx 0$)

Since 2010 – Beam energy scans to study QCD phase diagram: search for the 1st order phase transition and CEP at Intermediate T , high μ !

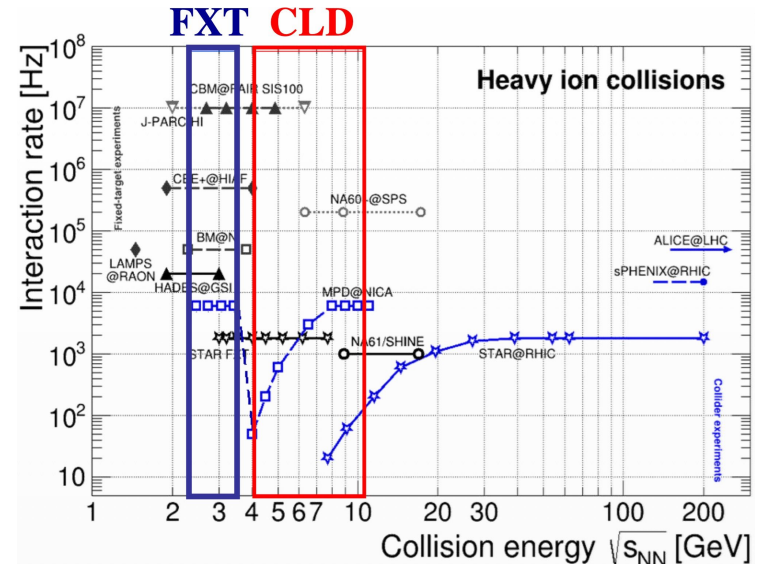
NICA: unique and complementary



- At $\mu_B \sim 0$, smooth crossover (lattice QCD + data)
- At large μ_B , we expect 1st order phase transition \rightarrow QCD critical point
- Thermal model indicates that highest baryon density is achieved at NICA energy
- Energy range $\sqrt{s_{NN}} < 6$ GeV \rightarrow most appropriate to search CEP

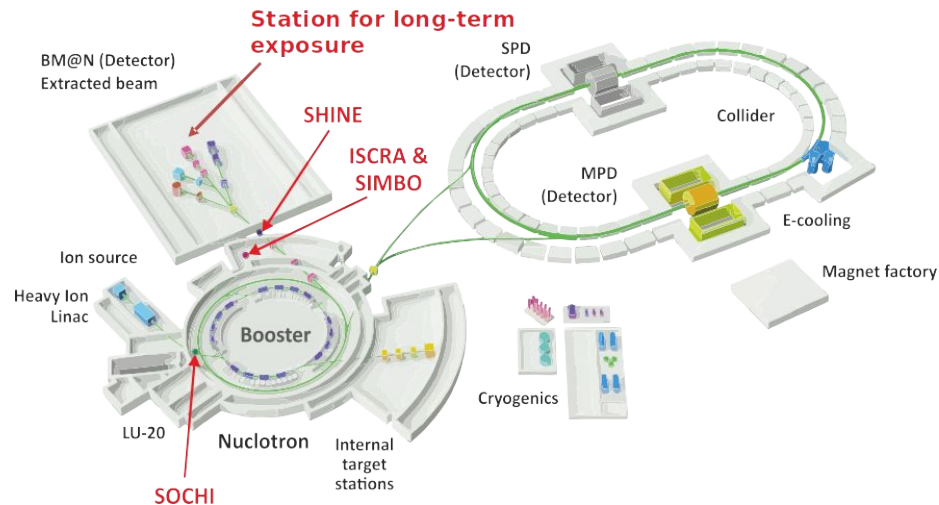
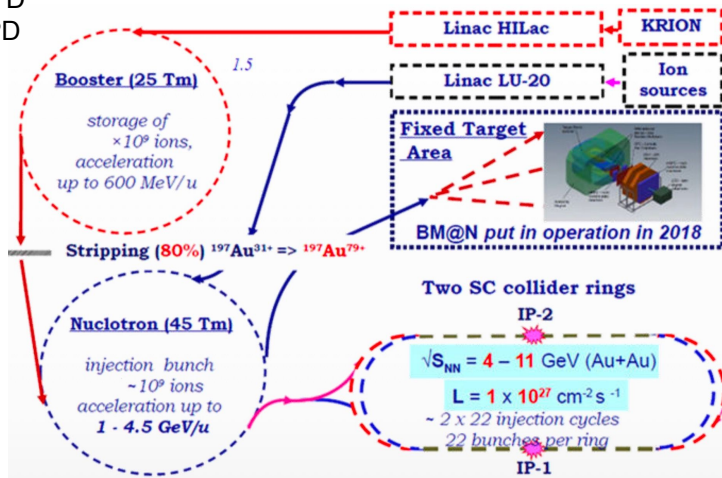
BM@N and MPD will study QCD Medium at extreme net baryon densities.

Many ongoing (NA61/SHINE, STAR-BES) and future experiments (CBM at FAIR) in the same energy range



MPD at NICA Complex in Dubna

- Two injection chains
 - Ion sources ($A/Z \leq 3$) → LINAC LU-20 (5 MeV/u) → Nuclotron
 - 1 ESIS KRION sources ($A/Z \leq 6$) → HILAc (3.24 MeV/u) → Booster
- SC Booster synchrotron
 - injection up to $2 \cdot 10^9$ accelerated up to ~ 600 MeV/u ions of $^{197}\text{Au}^{31+}$
- Nuclotron synchrotron
 - injection up to $1 \cdot 10^9$ ions accelerated up to 1 – 4.5 GeV/n
 - BM@N
- Two Collider superconducting storage rings
 - MPD
 - SPD
- ARIADNA



Megascience project in Russia, which is approaching its full commissioning:

- ❖ Baryonic Matter at Nuclotron (**BM@N**) – fixed-target experiment, first physics run Xe+CsI 2022–2023
- ❖ Multi-Purpose Detector (**MPD**) – start of operation in 2025–2026
- ❖ Spin Physics Detector (**SPD**) – operating on polarized deuterons later on
- ❖ Applied Research Infrastructure for Advanced Developments at NICA facility (**ARIADNA**)

NICA Accelerator Complex

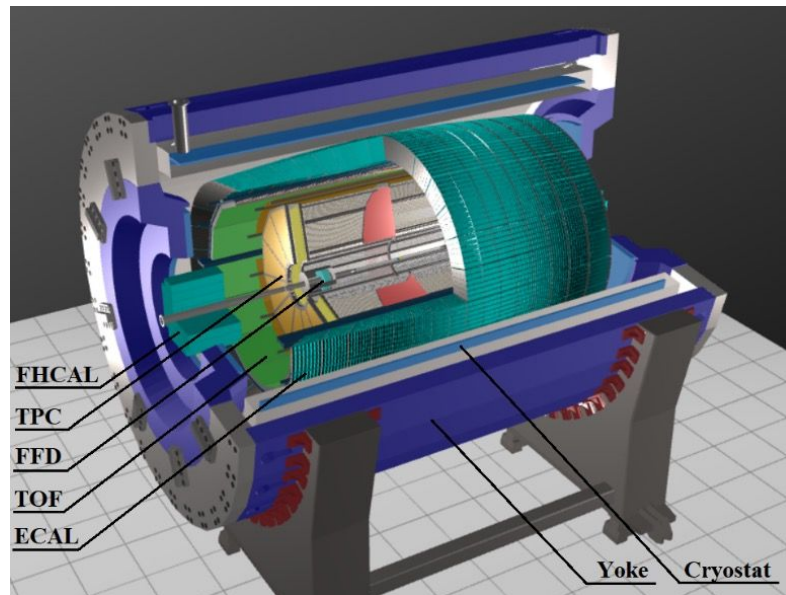


Multi-Purpose Detector (MPD) at NICA

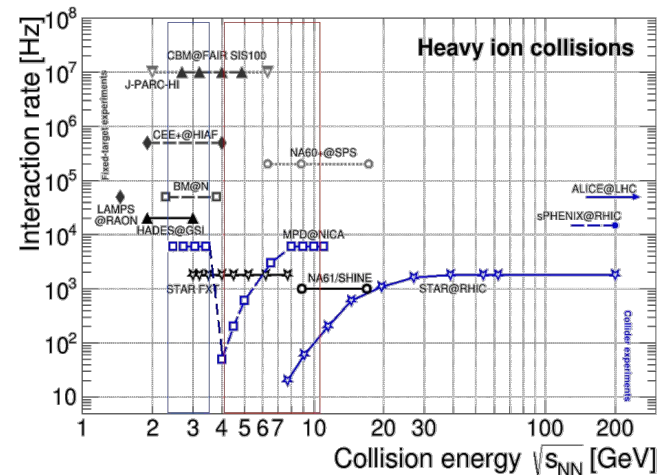
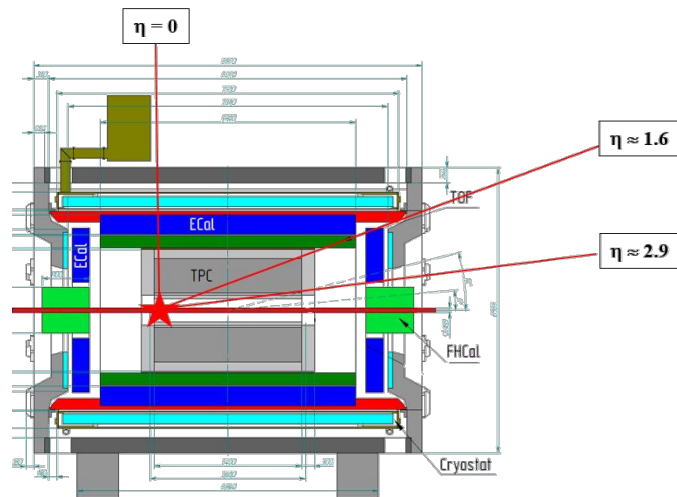
The central barrel of the MPD is built as a classical magnetic spectrometer with a full coverage in azimuthal angle ($|\Delta\phi| < 2\pi$) and a wide coverage in pseudorapidity ($|\Delta\eta| < 1.5$)

Main subsystems at Stage-I:

- ★ **TPC** ($\eta \leq 1.6$): charged particle tracking + momentum reconstruction + dE/dx identification
- ★ **TOF** ($\eta \leq 1.4$): charged particle identification
- ★ **ECal** ($2.9 < \eta < 1.4$): energy and PID for γ/e^\pm
- ★ **FHCAL** ($2 < \eta < 5$) and **FFD** ($2.9 < \eta < 3.3$): event triggering + event geometry



Fixed Target Operation



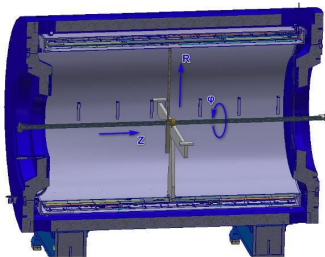
- MPD-CLD (Collider) and MPD-FXT (Fixed Target) options approved by accelerator department
- Collider mode: two beams, $\sqrt{s_{NN}} = 4\text{--}11$ GeV
- Fixed-target mode: one beam + thin wire (~ 100 μm) close to the edge of the MPD central barrel:
 - extends energy range of MPD to $\sqrt{s_{NN}} = 2.4\text{--}3.5$ GeV (overlap with HADES, BM@N and CBM)
 - high event rate

Expected beams at the first year(s) of operation (Stage-I):

- MPD-CLD: Xe/Bi + Xe/Bi at $\sqrt{s_{NN}} \sim 7$ GeV, reduced luminosity collision rate ~ 50 Hz
- MPD-FXT: Xe/Bi + W at $\sqrt{s_{NN}} \sim 3$ GeV

Detector Construction

SC Solenoid + Iron Yoke + Mapper



- Test cooling performed to 70°K in March 2024
- Start of cooling to LHe and magnetic field measurements in the second half of the 2024
- Magnetic field mapper is ready

Support structure



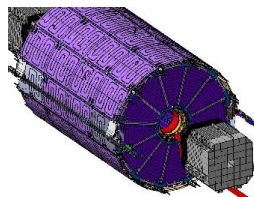
Carbon fiber support frame delivered and ready to use

TOF - ready



28 modules are produced and ready for installation

TPC - Central Tracking System



TPC cylinders, central membrane, service wheels, rails, readout chambers, gas system – ready; TPC gas volume assembly and HV/leakage tests – ongoing

- TPC + ECAL cooling systems commissioned in early 2025

ECal

Produced in consortium with China institutes



83% of calorimeter will be ready in 2024 the rest of the modules will be ready by the April 2025

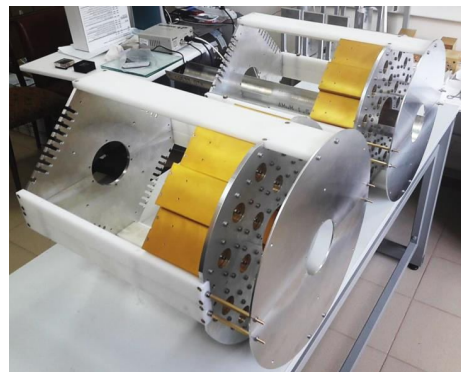
Forward subsystems in production

FHCal

FHCal assembled on the platform, ready to be installed in the Poles (modules are equipped with FEE)

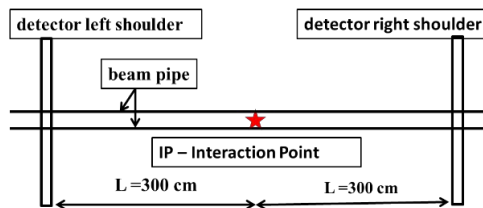
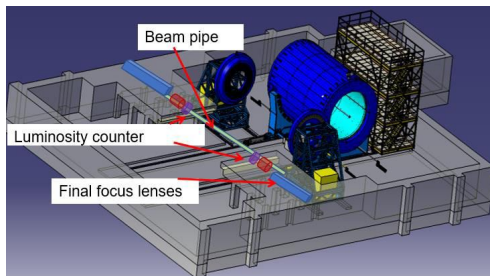


FFD
Cherenkov modules of FFDE and FFDW, mechanics for installation in container with beam pipe are available, Long term tests with cosmic rays & laser ongoing

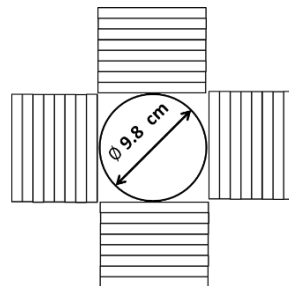


FHCAL modules have been produced and tested installation in autumn 2024

Beam and luminosity monitoring



Measurement of transverse sizes of the bunches
Transverse and longitudinal convergence of bunches
Vertices distribution along the beam



Assembly of the main components of the detector for the Run on the collider beam - June 2025

Mini BeBe

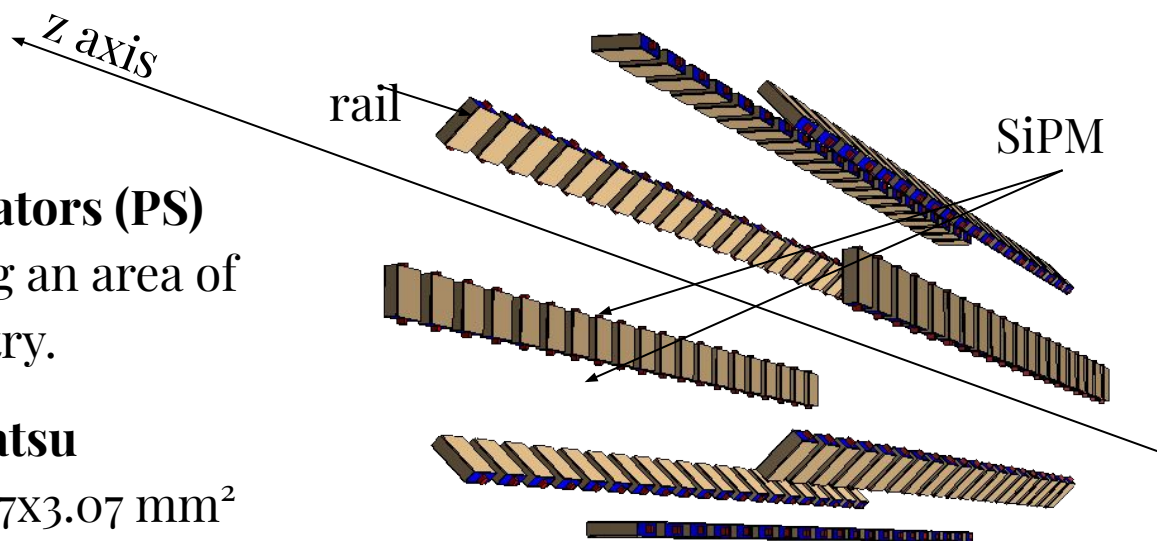
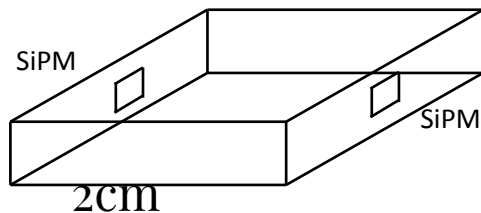
ITS-miniBeBe cooperation - development for different stages

- MiniBeBe detector was proposed as a wake-up trigger for TOF detector.
- Should be efficient for low multiplicity events like p+p, p+A and A+A.
In which other systems are not efficient
- Designed to be used only in Phase 0, before ITS installation

MiniBeBe - Geometry

It consist on **160 plastic scintillators (PS)**
EJ232 - $20 \times 20 \times 5 \text{ mm}^3$ \gg covering an area of
 64000 mm^2 in a coaxial symmetry.

Each **PS** has two **SiPM Hamamatsu**
S13360-3050PE at each side $3.07 \times 3.07 \text{ mm}^2$



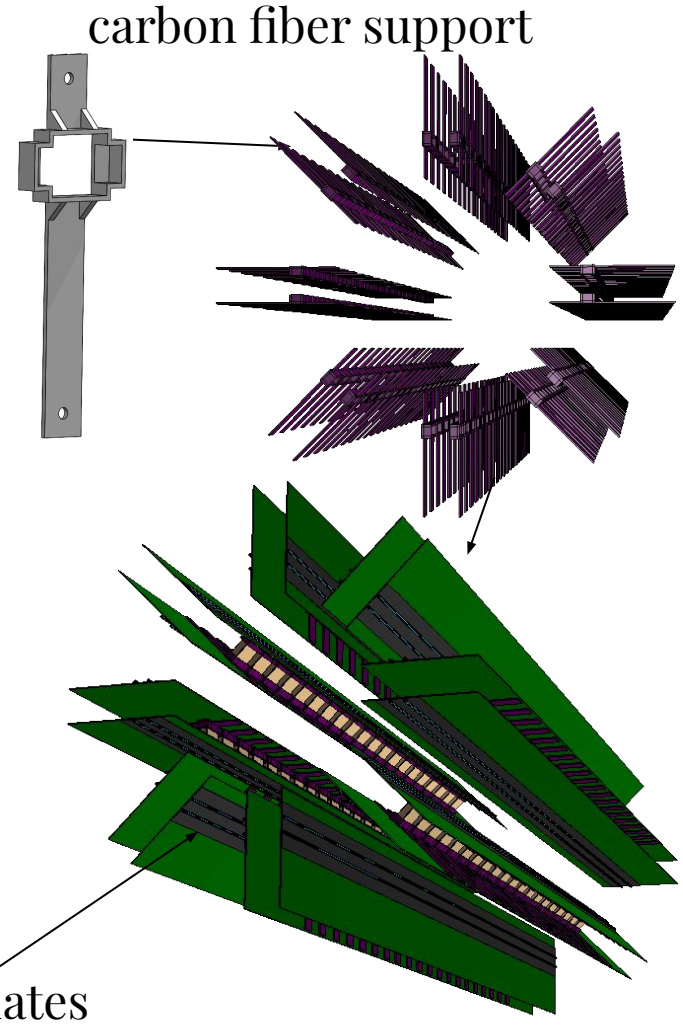
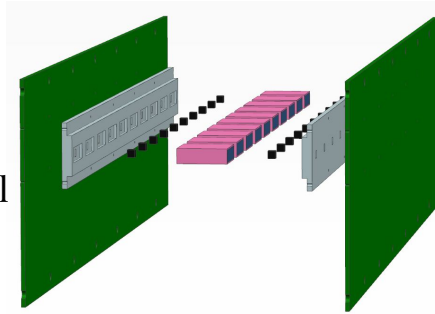
MiniBeBe - Geometry

The PCBs are connected to the SiPMs at each side of the PS providing an **H-shaped** rail (80 x 800 mm²).

Each SiPM-PS-SiPM element is fixed to the PCBs with a carbon fiber supports.

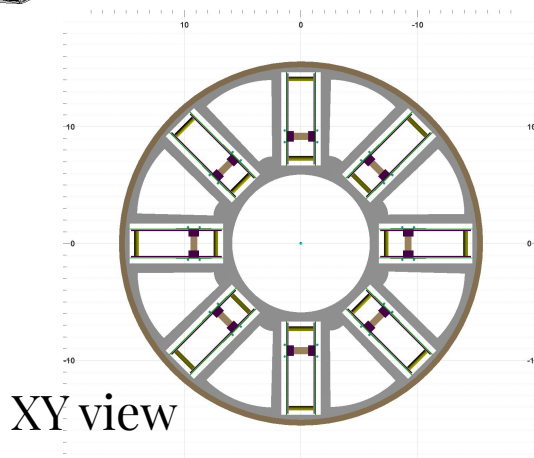
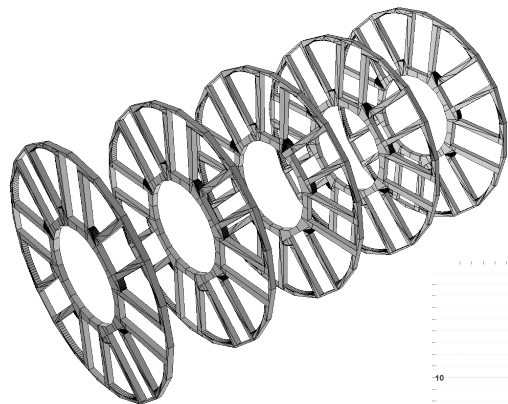
Attached to PCBs are the Carbon Fiber cold plates (same of ITS)

exploded view
diagram of H-rail

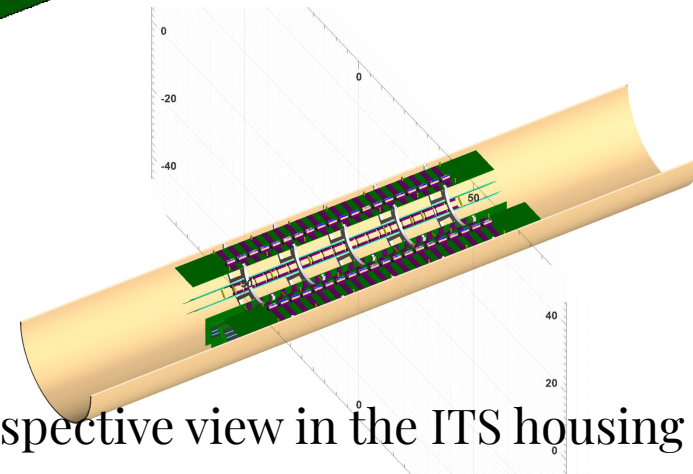
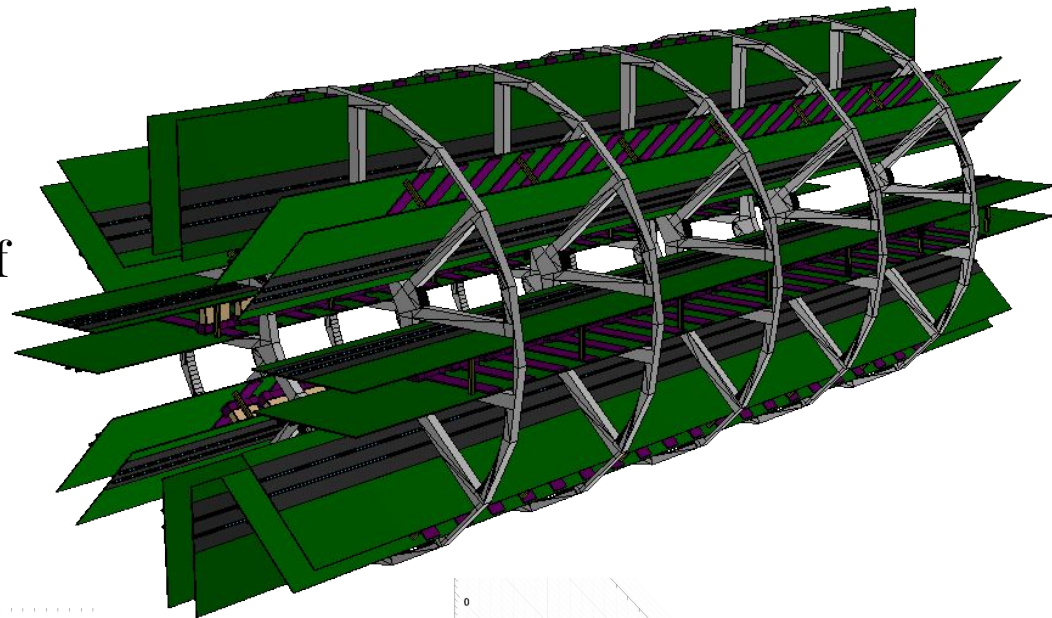


MiniBeBe - Geometry

Modules are fixed to the Inner Barrel of the ITS with Aluminum flanges



XY view



Perspective view in the ITS housing

Xe+Xe collisions, Probability to 1 hit as a function of z - position

Probability to have 1 hit at each ring per event - XeXe $\sqrt{s_{NN}} = 9.2 \text{ GeV}$

DCM-QGSM-SMM

π, K, p, e, μ

$b \in (0,2) \text{ fm}$

$b \in (2,4) \text{ fm}$

$b \in (4,6) \text{ fm}$

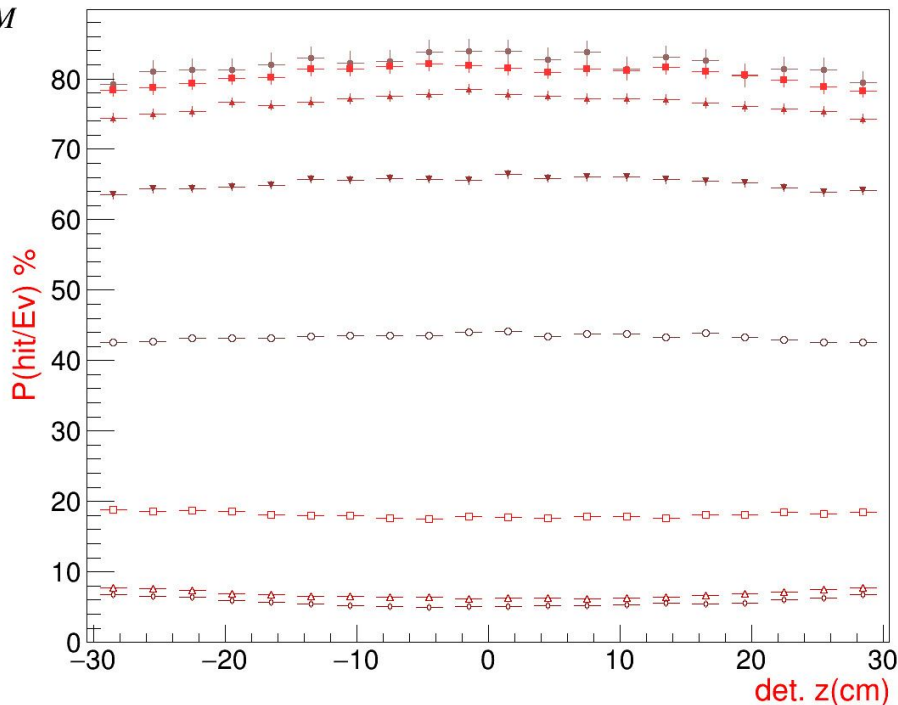
$b \in (6,8) \text{ fm}$

$b \in (8,10) \text{ fm}$

$b \in (10,12) \text{ fm}$

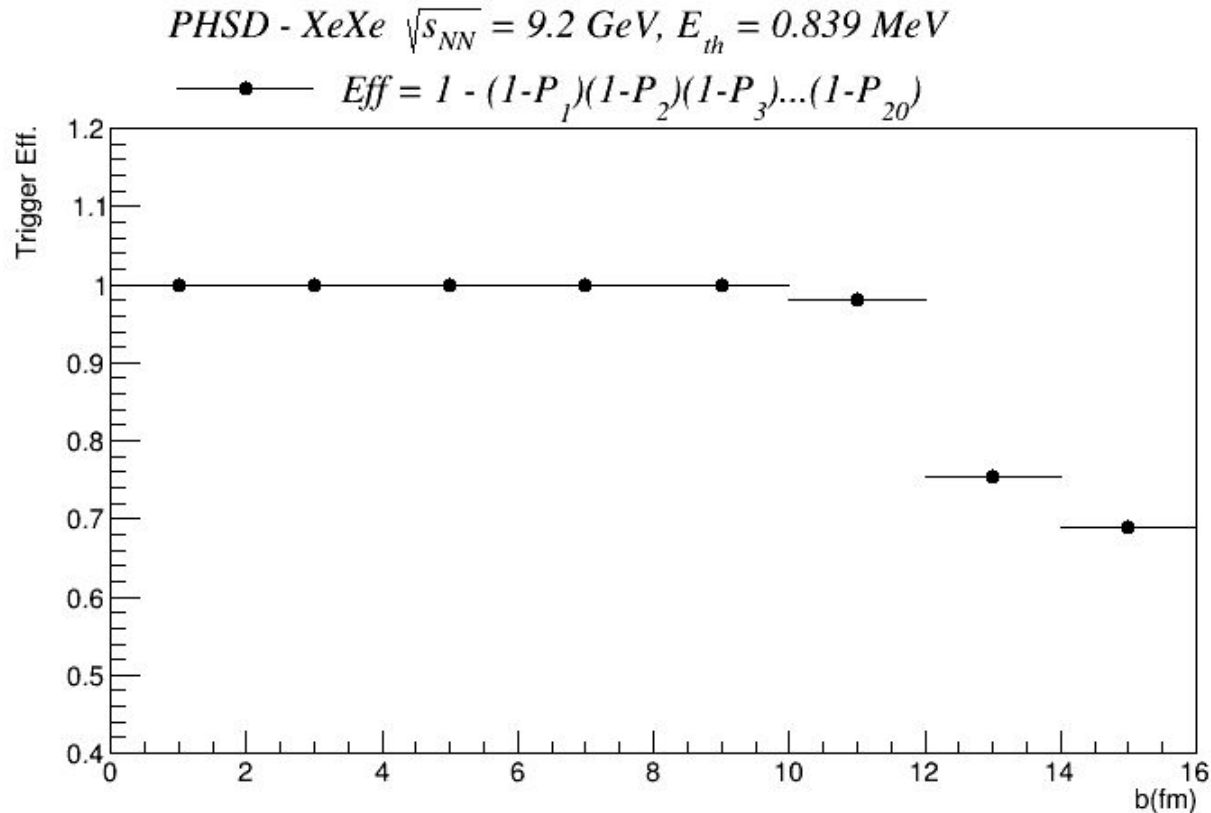
$b \in (12,14) \text{ fm}$

$b \in (14,16) \text{ fm}$



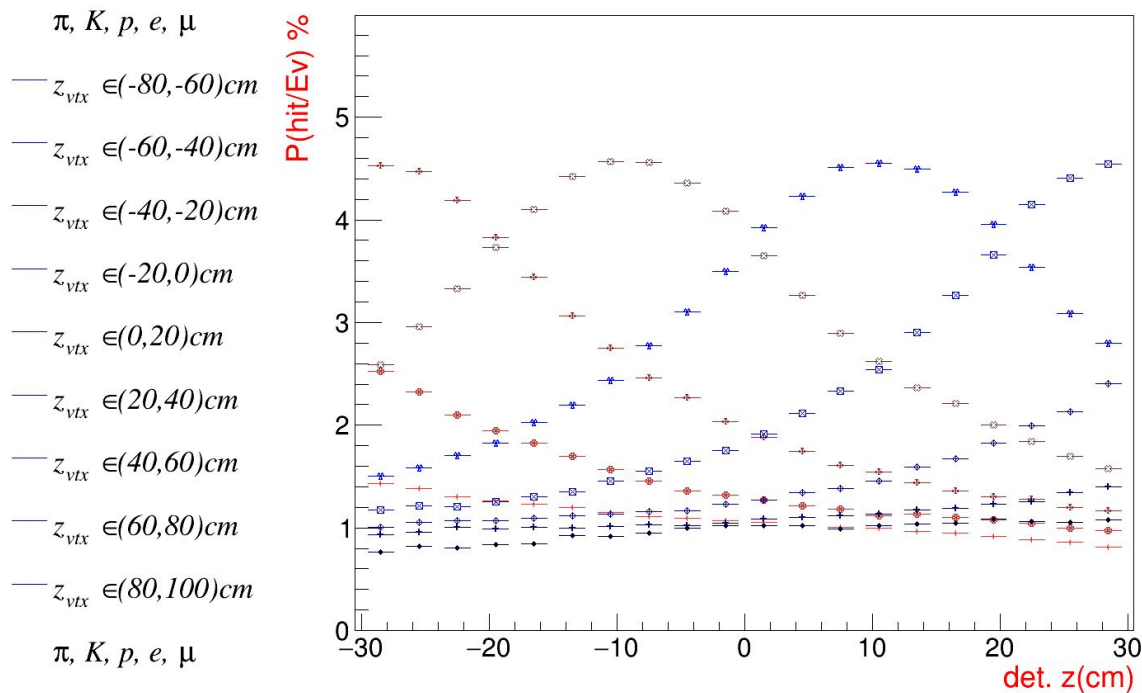
At least one charged
MbbPoint at each ring,
for events with different
impact parameter

Trigger Efficiency as a function of Impact Parameter for Xe+Xe



p+p collisions, Probability to 1 hit as a function of z - position

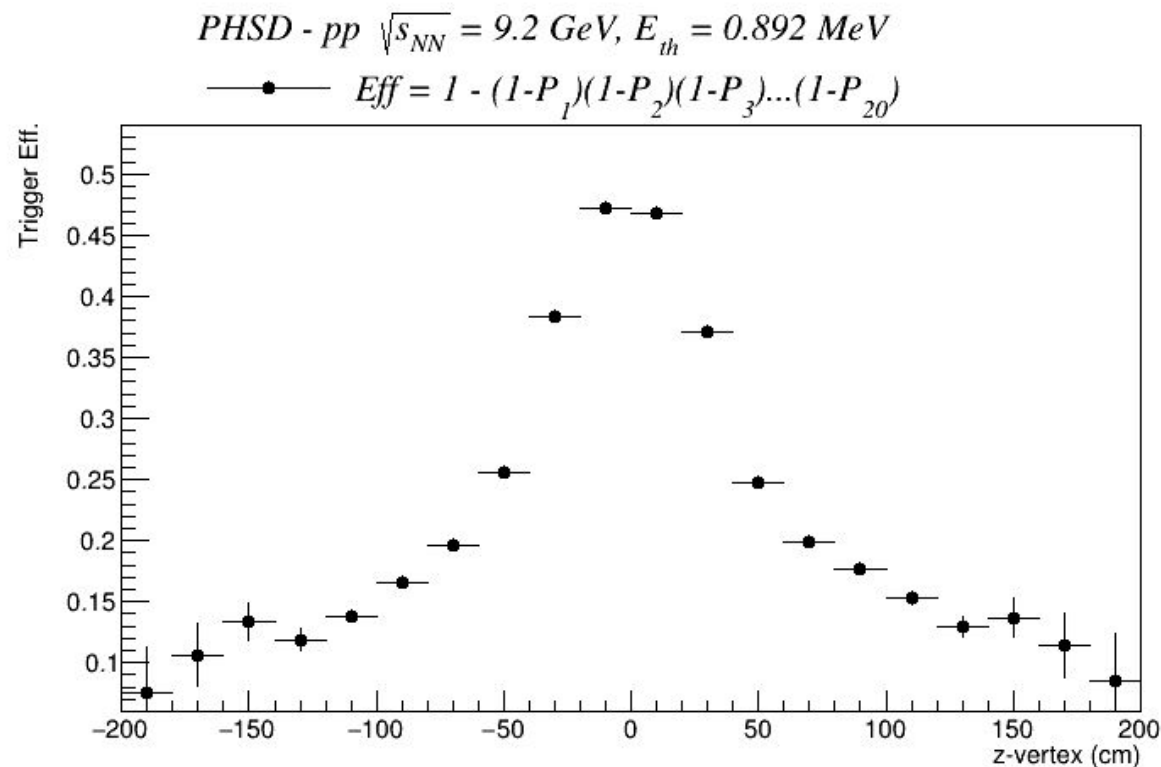
Probability to have 1 hit at each ring per event - pp $\sqrt{s_{NN}} = 9.2 \text{ GeV}$



The smallest collision system

At least one charged MbbPoint at each ring, for events with different primary vertex position

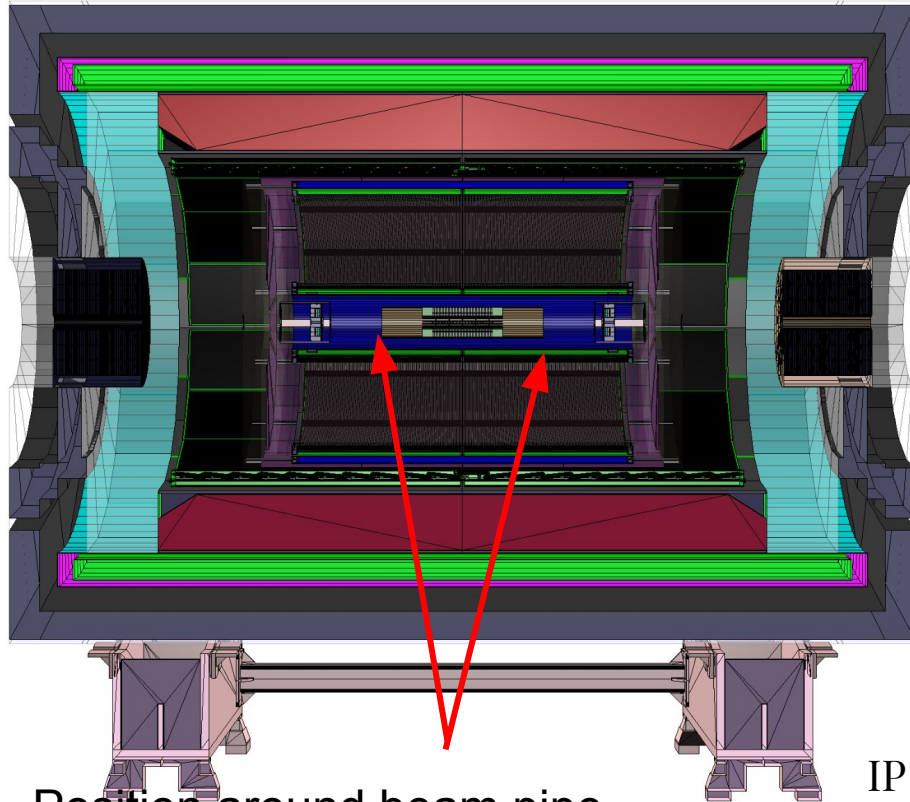
Trigger Efficiency as a function of Impact Parameter for p+p



Trigger efficiency is not uniform

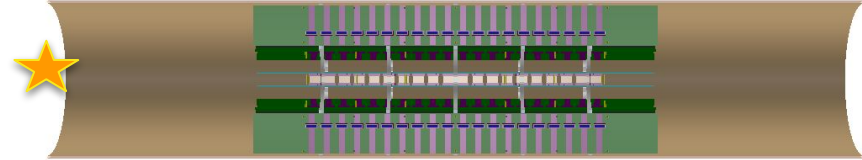
Trigger Efficiency > 35%
only for events with
primary vertex \in
(-40,40)cm

Position in the MPD has been tested for Fixed Target Mode

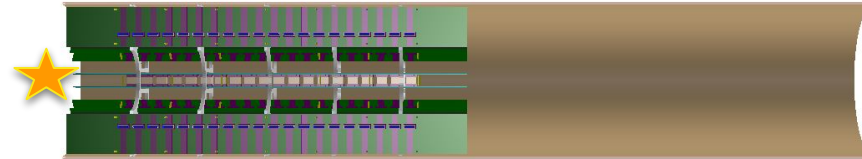


Position around beam pipe
in Central Position

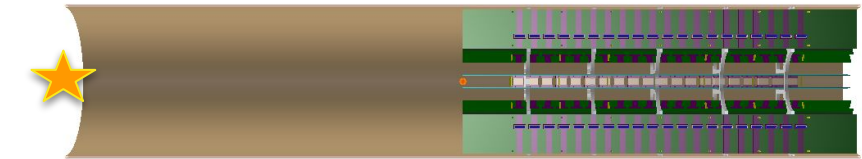
CENTRAL POSITION



LEFT POSITION



RIGHT POSITION



IP $z = -85\text{cm}$ distance between IP and center of MBB:
central $\Rightarrow 85\text{cm}$, left $\Rightarrow 45\text{ cm}$ and right $\Rightarrow 125\text{cm}$

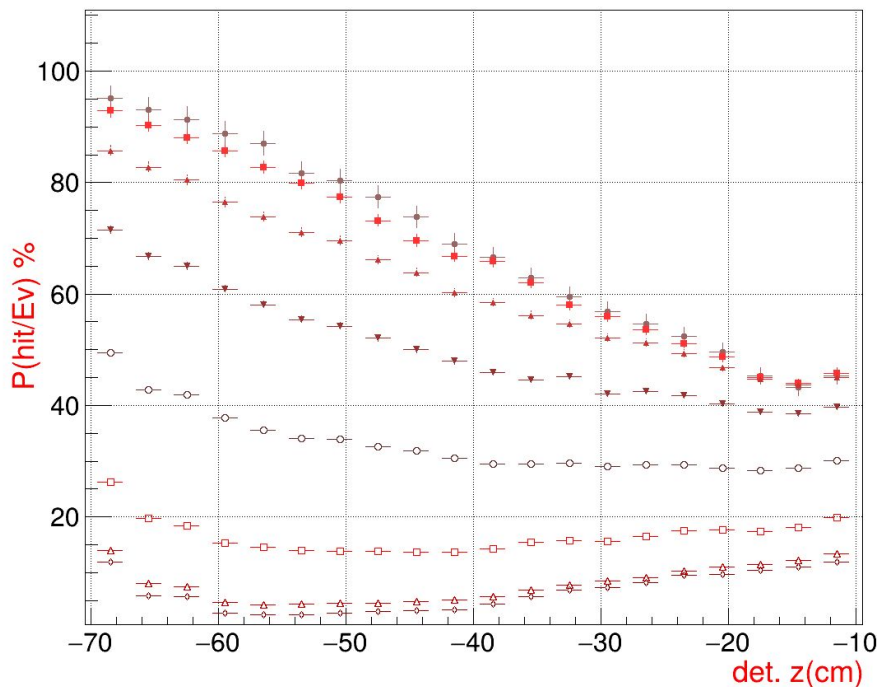
Probability to 1 hit at each ring as a function of impact parameter

Probability to have 1 hit at each ring per event - $\text{Xe}^{124} + \text{W}$, $T = 2.5 \text{ GeV}$, Left Position

UrQMD

π, K, p, e, μ

- $b \in (0, 2) \text{ fm}$
- $b \in (2, 4) \text{ fm}$
- $b \in (4, 6) \text{ fm}$
- $b \in (6, 8) \text{ fm}$
- $b \in (8, 10) \text{ fm}$
- $b \in (10, 12) \text{ fm}$
- $b \in (12, 14) \text{ fm}$
- $b \in (14, 16) \text{ fm}$



At least one charged
MbbHit at each ring, for
LEFT Position

Each ring corresponds to
position on z direction of
the plastic scintillators

Probability to 1 hit as a function of impact parameter

Probability to have 1 hit at each ring per event - $\text{Xe}^{124} + \text{W}$, $T = 2.5 \text{ GeV}$, Central Position

UrQMD

π, K, p, e, μ

$b \in (0,2) \text{ fm}$

$b \in (2,4) \text{ fm}$

$b \in (4,6) \text{ fm}$

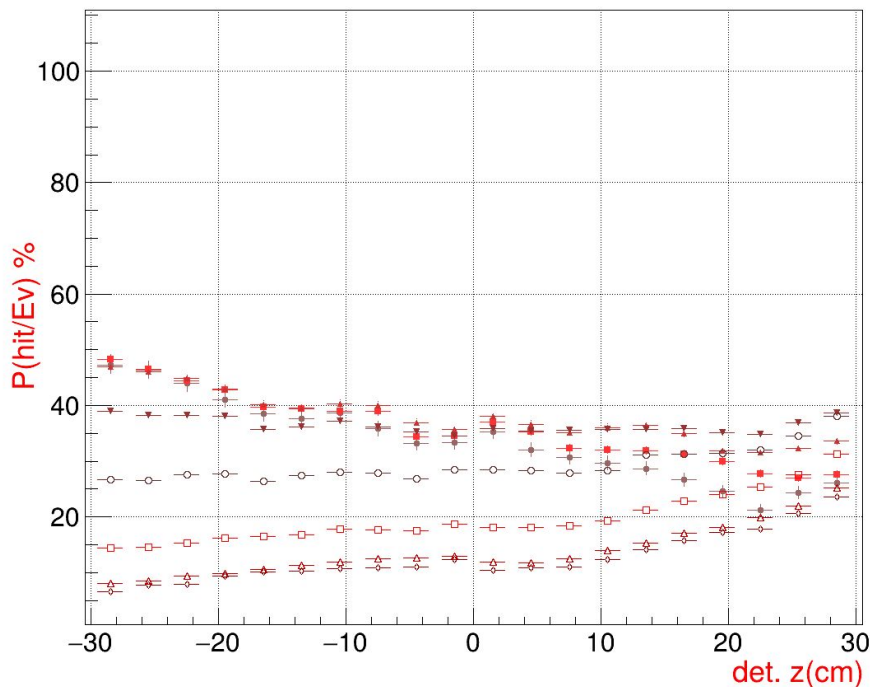
$b \in (6,8) \text{ fm}$

$b \in (8,10) \text{ fm}$

$b \in (10,12) \text{ fm}$

$b \in (12,14) \text{ fm}$

$b \in (14,16) \text{ fm}$



At least one charged
MbbHit at each ring, for
CENTRAL Position

Probability to 1 hit as a function of impact parameter

Probability to have 1 hit at each ring per event - $\text{Xe}^{124} + \text{W}$, $T = 2.5 \text{ GeV}$, Right Position

UrQMD

π, K, p, e, μ

$b \in (0,2) \text{ fm}$

$b \in (2,4) \text{ fm}$

$b \in (4,6) \text{ fm}$

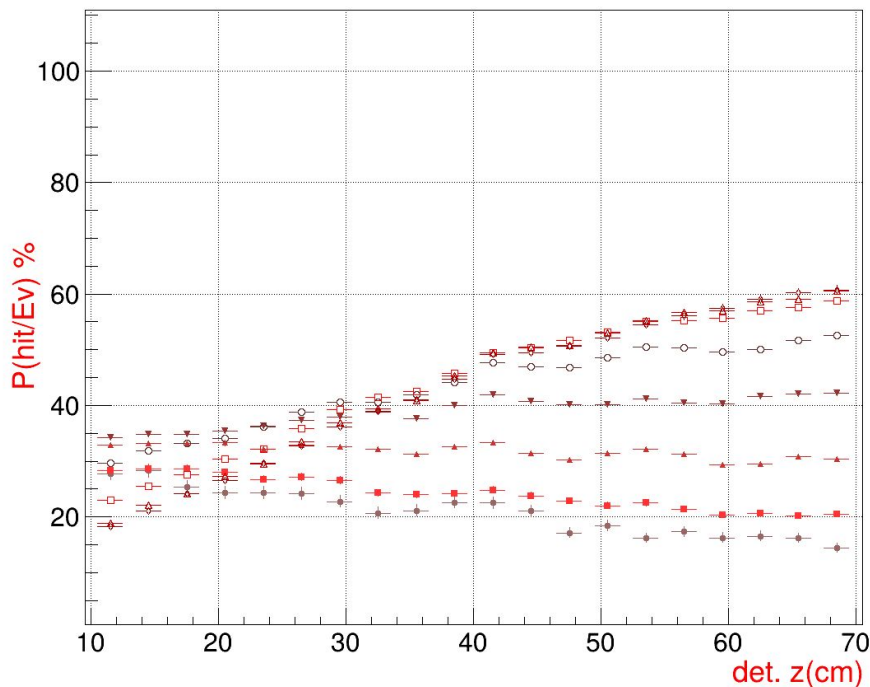
$b \in (6,8) \text{ fm}$

$b \in (8,10) \text{ fm}$

$b \in (10,12) \text{ fm}$

$b \in (12,14) \text{ fm}$

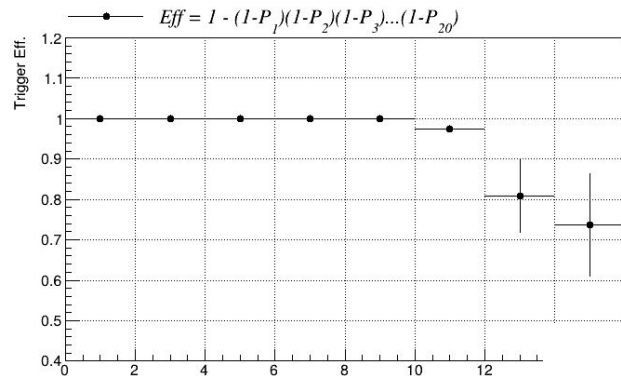
$b \in (14,16) \text{ fm}$



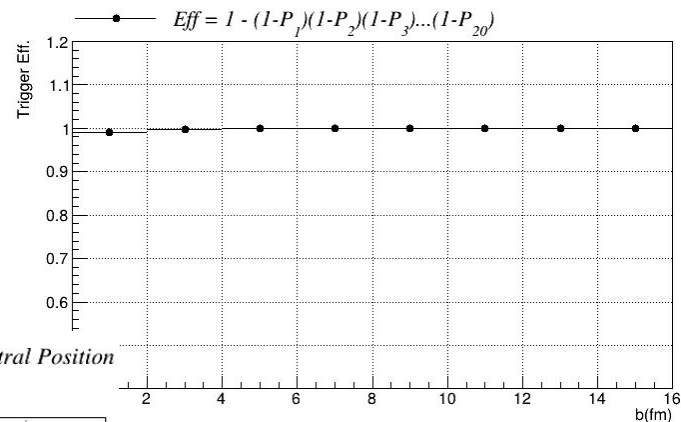
At least one charged
MbbHit at each ring, for
RIGHT Position

Trigger Efficiency as a function of Impact Parameter with 1 hit

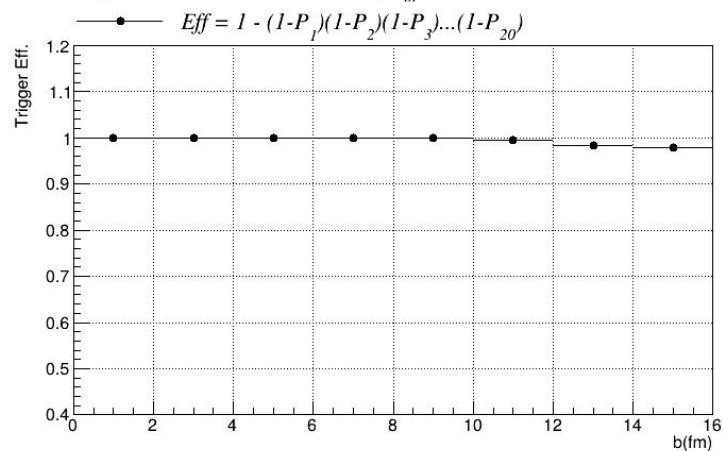
UrQMD - $Xe^{124} + W T = 2.5 \text{ GeV}$, $E_{th} = 0.839 \text{ MeV}$ - Left Position



UrQMD - $Xe^{124} + W T = 2.5 \text{ GeV}$, $E_{th} = 0.839 \text{ MeV}$ - Right Position

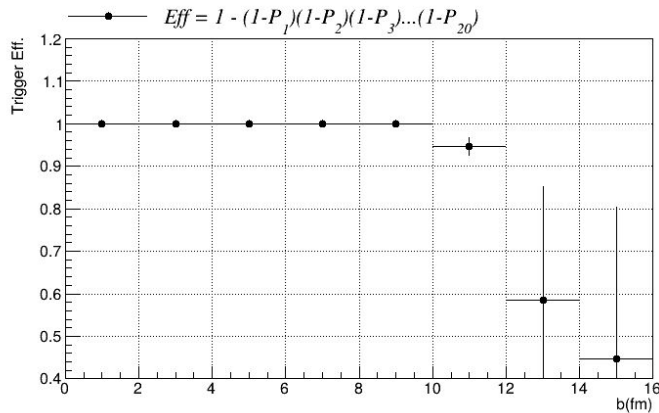


UrQMD - $Xe^{124} + W T = 2.5 \text{ GeV}$, $E_{th} = 0.839 \text{ MeV}$ - Central Position

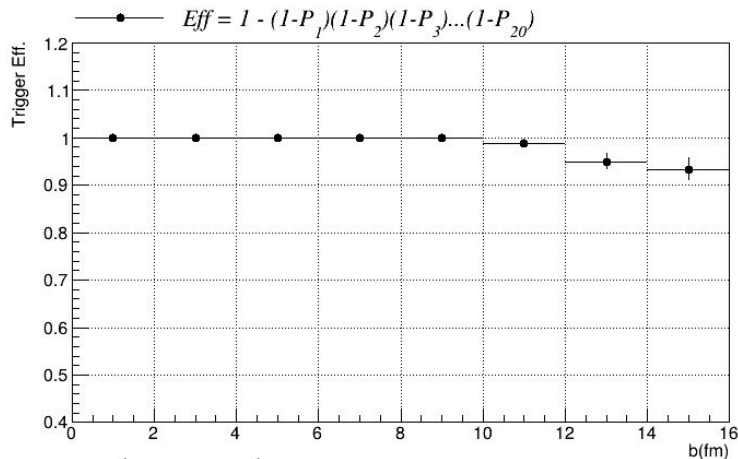


Trigger Efficiency as a function of b with 1 hit at each side

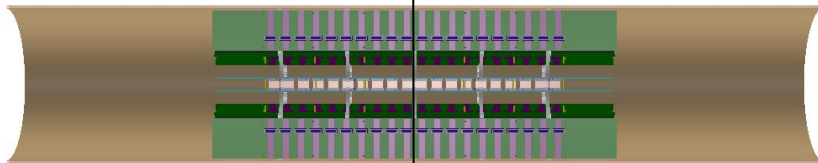
UrQMD - $Xe^{124} + WT = 2.5 \text{ GeV}$, $E_{th} = 0.839 \text{ MeV}$ - Left Position



UrQMD - $Xe^{124} + WT = 2.5 \text{ GeV}$, $E_{th} = 0.839 \text{ MeV}$ - Central Position

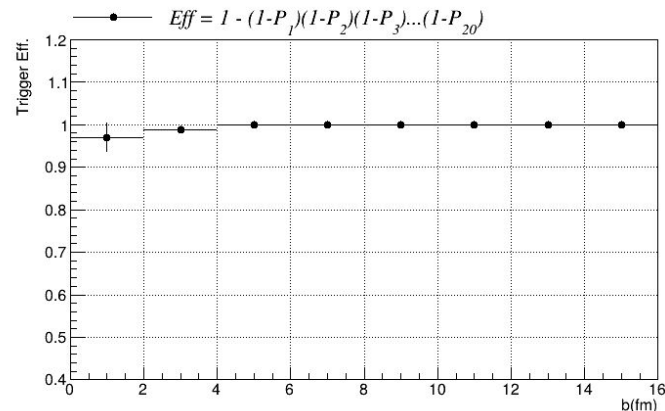


Modules are divided: read out is independent



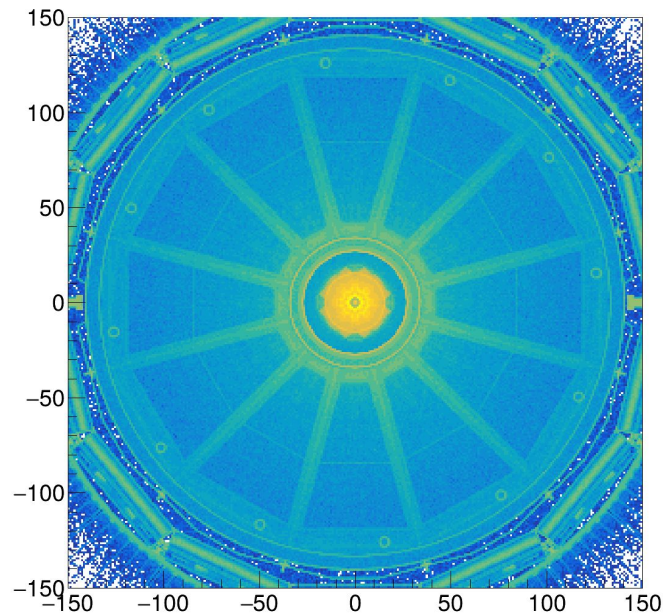
We can get the efficiency with 1 hit at each half

UrQMD - $Xe^{124} + WT = 2.5 \text{ GeV}$, $E_{th} = 0.839 \text{ MeV}$ - Right Position



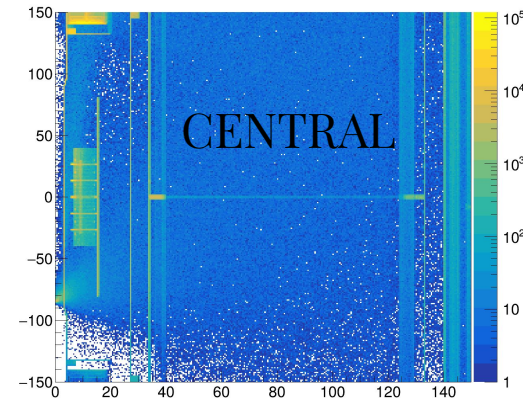
Secondary particle production

XvsY Secondary

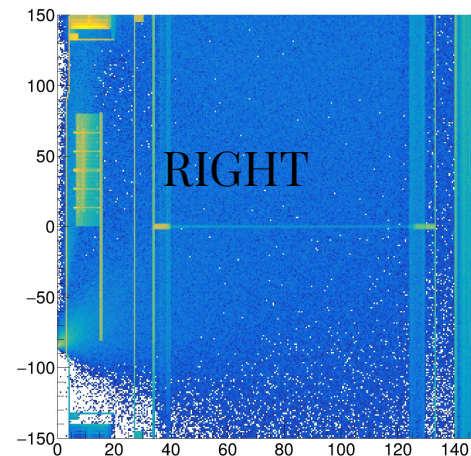


Study of secondary particles in the other detectors is work in progress

RvsZ Secondary

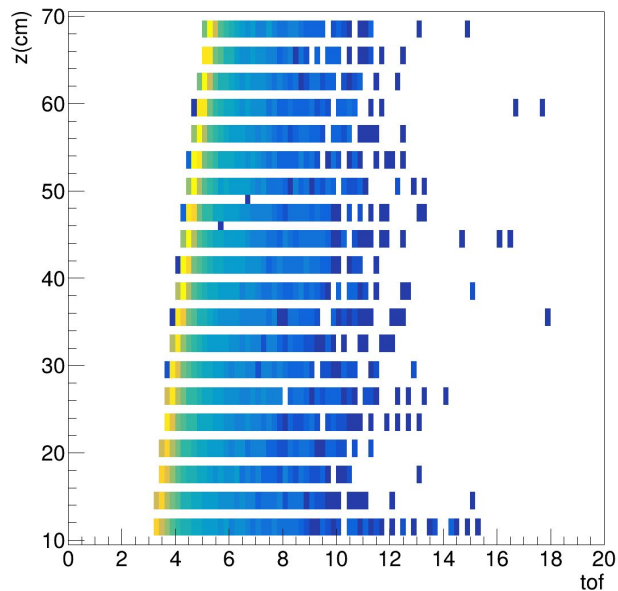


RvsZ Secondary

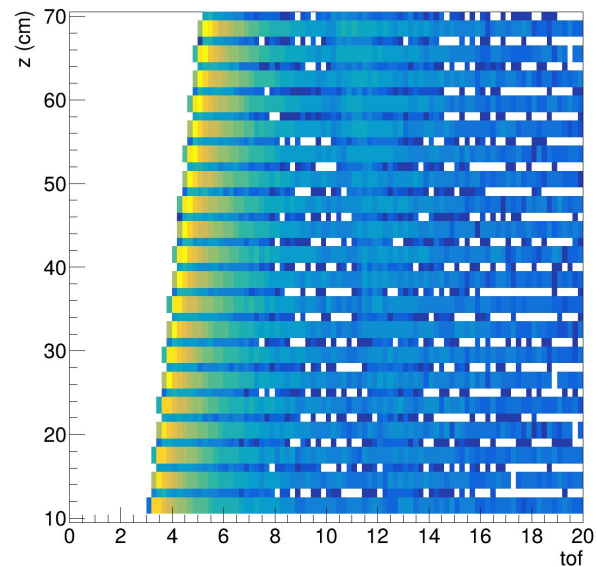


Reaching Time

Primary particles



Secondary particles



Material Budget

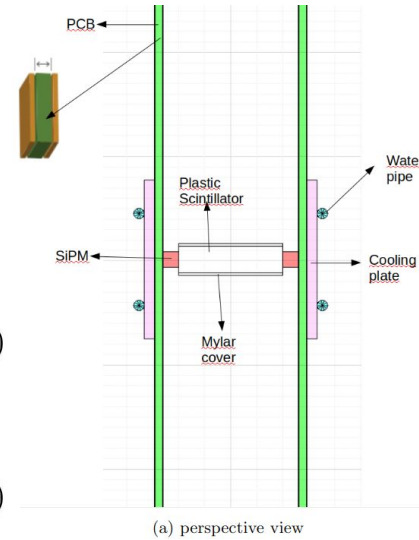
Radiation Length

The radiation length can be approximated by:

$$X_0 = \frac{716.4 \times A}{Z(Z+1) \ln\left(\frac{287}{\sqrt{Z}}\right)} \left[\frac{g}{cm^3} \right] \quad (1)$$

For different materials:

$$\frac{W_0}{X_0} = \sum_i \frac{W_i}{X_i} \quad (2)$$



Element	Dimensions
Plastic Scintillator	20x20x5 mm ³
SiPM	3x3x3 mm ³
Mylar cover	thickness = 0.5 mm
FR4	800x100x1.4 mm ³
Copper	800x10x0.1 mm ³
Cooling plate	800x30.6x2 mm ³
Water pipe	radius = 1.025 mm

(b) Dimensions of material in the rail used for material budget simulation.

Element	X_0 (g/cm ²)	ρ (g/cm ³)	\bar{X} (cm)	Average Mat. Budget %
Plastic Scintillator & SiPM	43.3886	1.032	0.57	1.31
Mylar	39.69	1.39	0.07	0.25
FR4	288.67	1.86	1.25	0.80
Copper	12.86	8.96	0.10	6.83
Carbon-Fiber	42.11	1.383	1.30	3.09
air	1.205E-3	36.66	7.08	0.02
water	35.758	1.	0.253	0.7

Table 1: Radiation Length X_0 and density ρ of materials used in simulation. Also is shown the average distance \bar{X} traveled by particles on each material and the corresponding material budget.

Material Budget

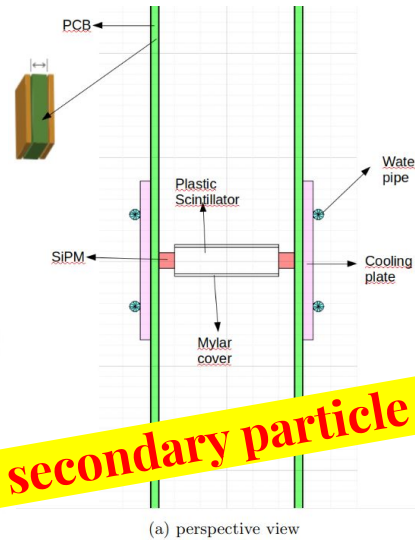
Radiation Length

The radiation length can be approximated by:

$$X_0 = \frac{716.4 \times A}{Z(Z+1) \ln\left(\frac{287}{\sqrt{Z}}\right)} \left[\frac{\text{g}}{\text{cm}^3} \right] \quad (1)$$

For different materials:

$$\frac{W_0}{X_0} = \sum \frac{W_i}{X_i}$$



Element	Dimensions
Plastic Scintillator	5 mm ³
Copper	800x10x0.1 mm ³
Cooling plate	800x30.6x2 mm ³
Water pipe	radius = 1.025 mm

(b) Dimensions of material in the rail used for material budget simulation.

Material	X_0 (cm)	ρ (g/cm ³)	\bar{X} (cm)	Average Mat. Budget %
Plastic Scintillator	43.3886	1.032	0.57	1.31
Mylar	39.69	1.39	0.07	0.25
FR4	288.67	1.86	1.25	0.80
Copper	12.86	8.96	0.10	6.83
Carbon-Fiber	42.11	1.383	1.30	3.09
air	1.205E-3	36.66	7.08	0.02
water	35.758	1.	0.253	0.7

**How is going to affect tracking the secondary particle production!!!
Studies under development**

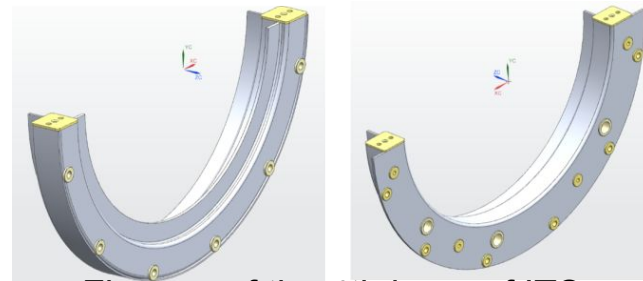
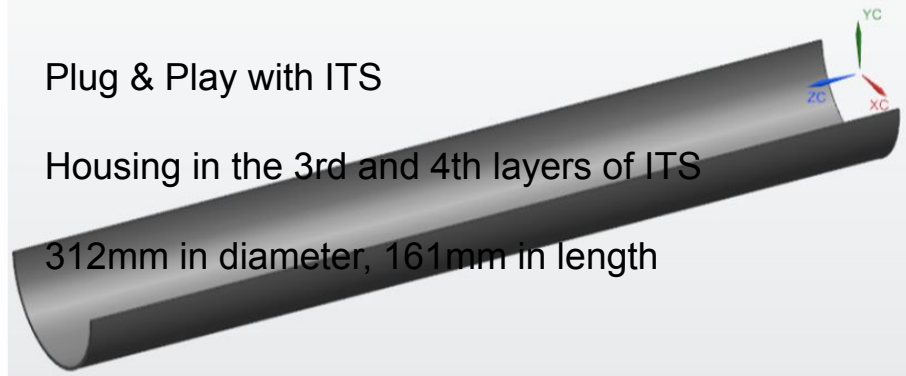
Table 1: Radiation Length X_0 and density ρ of materials used in simulation. Also is shown the average distance \bar{X} traveled by particles on each material and the corresponding material budget.

Mechanical support - Plug & Play MPD-ITS Mechanical Support

Plug & Play with ITS

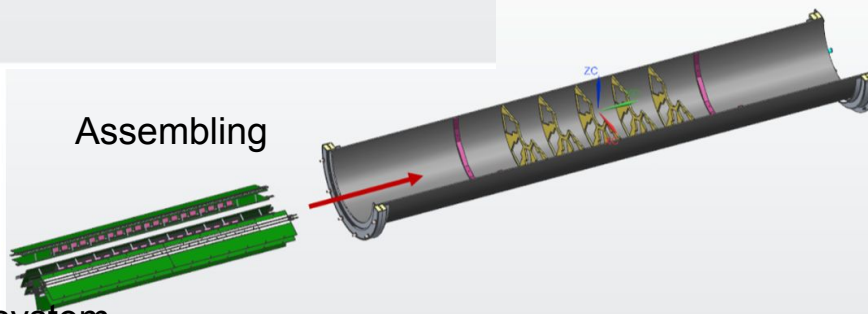
Housing in the 3rd and 4th layers of ITS

312mm in diameter, 161mm in length

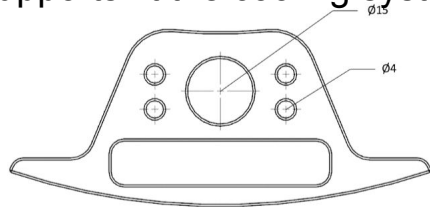


Flanges of the 4th layer of ITS were redesigned
Bushings of 9.3mm

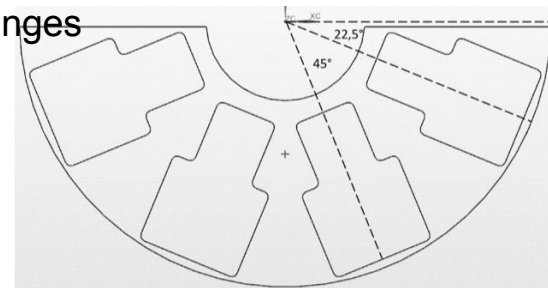
Assembling



Supports fit the cooling system

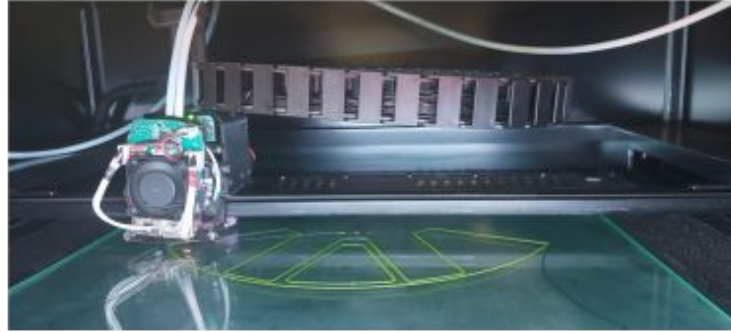


Electronic modules fixed with flanges



Mechanical Support

Prototype -printed at JINR



3D printing

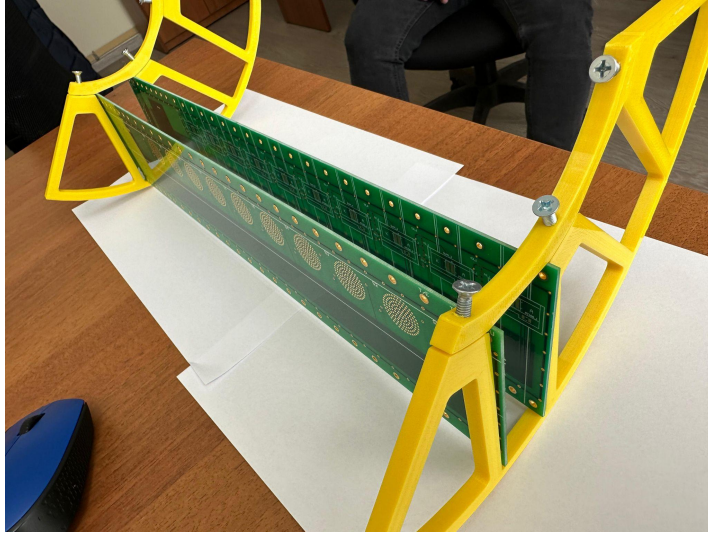


Filaments

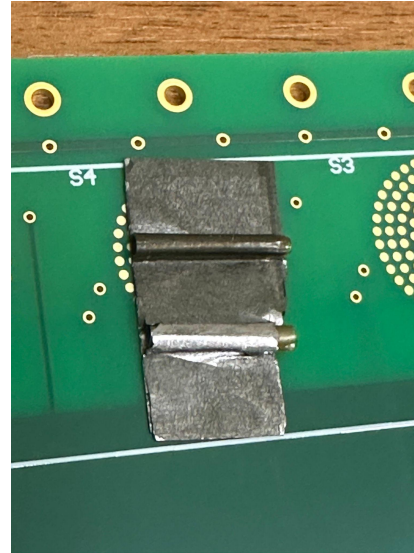


Flanges for rails support 32

Prototype - half module



Half module fixed with the flanges



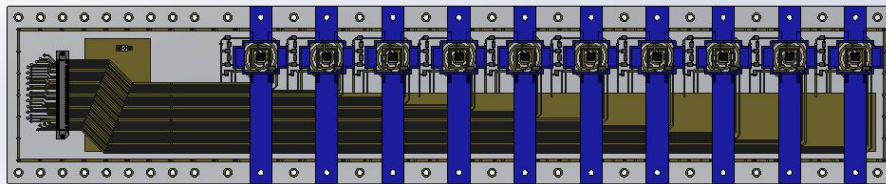
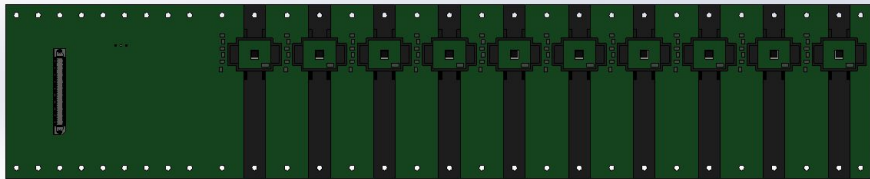
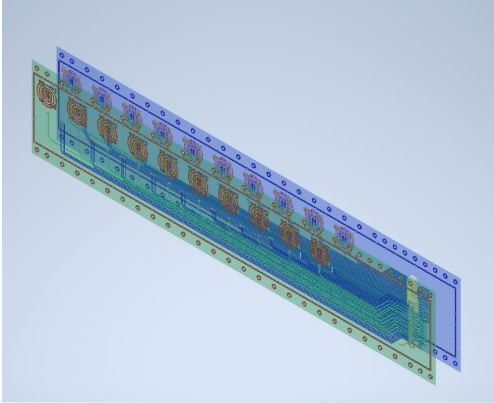
Cooling plates superposition



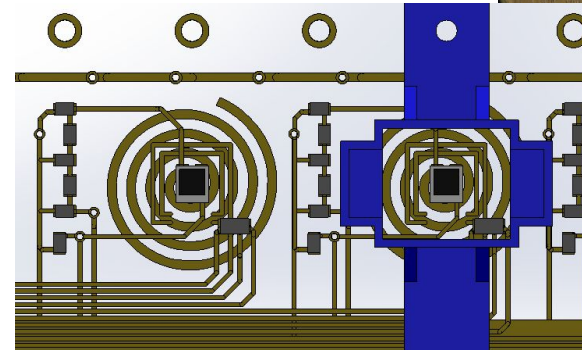
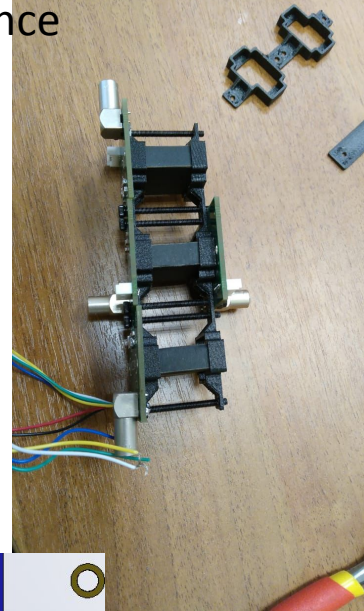
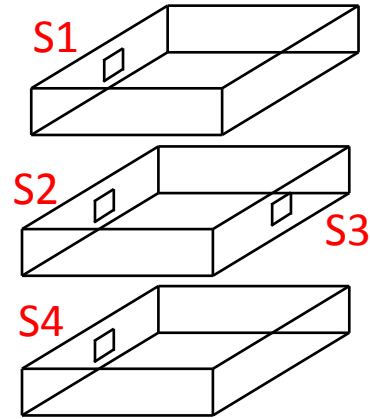
Frontal view, PS and screws

Electronic Module

Electronic board right and left
for 10 plastic scintillators. Half
module



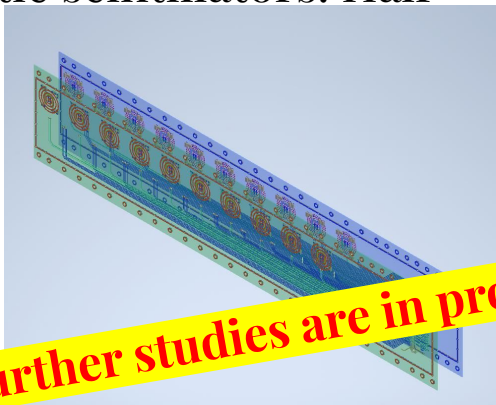
Array to test time coincidence



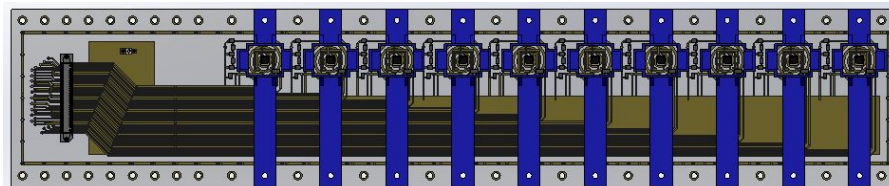
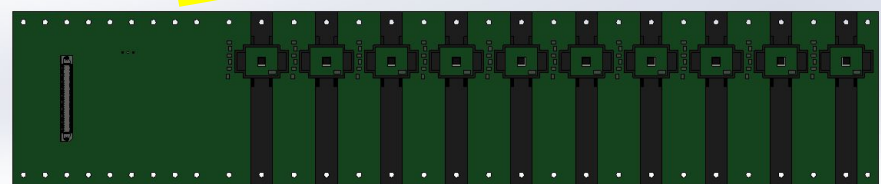
Circular copper heatsink that
connects the SiPM to the cooling
plate

Electronic Module

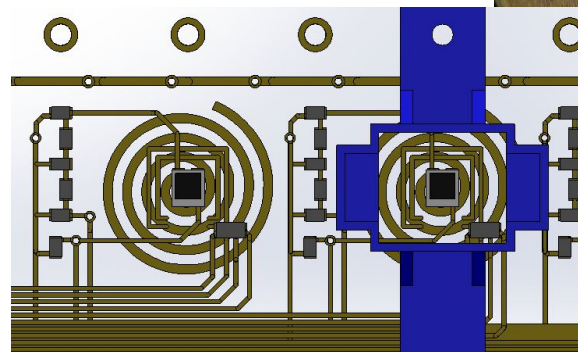
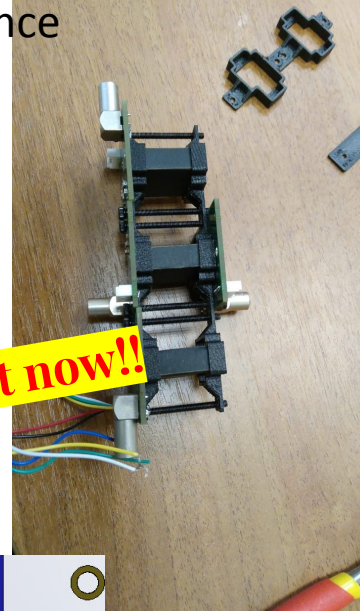
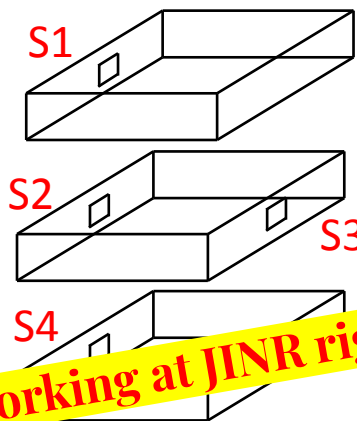
Electronic board right and left for 10 plastic scintillators. Half module



Further studies are in progress by team working at JINR right now!!



Array to test time coincidence



Circular copper heatsink that connects the SiPM to the cooling plate

Multi-Purpose Detector (MPD) Collaboration



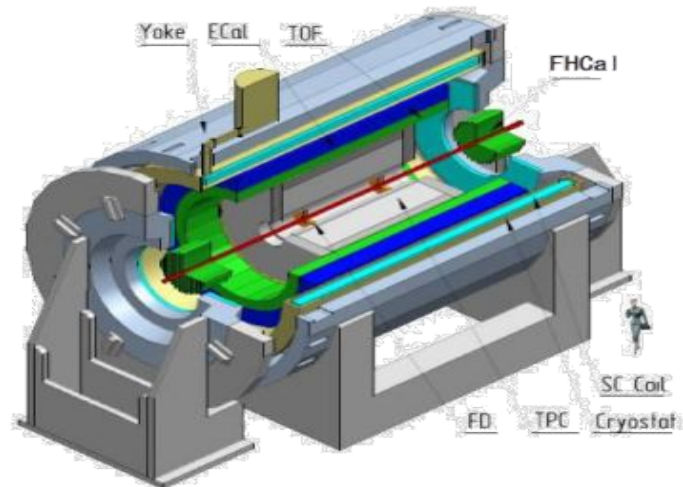
*MPD International Collaboration was established in 2018
to construct, commission and operate the detector*

12 Countries, >500 participants, 38 Institutes and JINR

Organization

Acting Spokesperson: Victor Riabov
Deputy Spokespersons: Zebao Tang, Arkadiy Taranenko
Institutional Board Chair: Alejandro Ayala
Project Manager: Slava Golovatyuk

Joint Institute for Nuclear Research, Dubna ;
A. Alikhanyan National Lab of Armenia, Yerevan, Armenia;
SSI "Joint Institute for Energy and Nuclear Research – Sosny" of the National
Academy of Sciences of Belarus, Minsk, Belarus
University of Plovdiv, Bulgaria;
Tsinghua University, Beijing, China;
University of Science and Technology of China, Hefei, China;
Huzhou University, Huzhou, China;
Institute of Nuclear and Applied Physics, CAS, Shanghai, China;
Central China Normal University, China;
Shandong University, Shandong, China;
University of Chinese Academy of Sciences, Beijing, China;
University of South China, China;
Three Gorges University, China;
Institute of Modern Physics of CAS, Lanzhou, China;
Tbilisi State University, Tbilisi, Georgia;
Institute of Physics and Technology, Almaty, Kazakhstan;
Benemérita Universidad Autónoma de Puebla, Mexico;
Centro de Investigación y de Estudios Avanzados, Mexico;
Instituto de Ciencias Nucleares, UNAM, Mexico;
Universidad Autónoma de Sinaloa, Mexico;
Universidad de Colima, Mexico;
Universidad de Sonora, Mexico;
Universidad Michoacana de San Nicolás de Hidalgo, Mexico
Institute of Applied Physics, Chisinev, Moldova;
Institute of Physics and Technology, Mongolia;

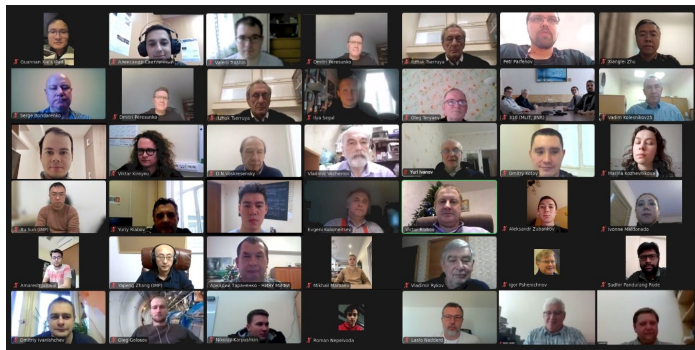


Belgorod National Research University, Russia;
Institute for Nuclear Research of the RAS, Moscow, Russia;
High School of Economics University, Moscow, Russia
National Research Nuclear University MEPhI, Moscow, Russia;
Moscow Institute of Science and Technology, Russia;
North Osetian State University, Russia;
National Research Center "Kurchatov Institute", Russia;
Peter the Great St. Petersburg Polytechnic University Saint Petersburg, Russia;
Plekhanov Russian University of Economics, Moscow, Russia;
St. Petersburg State University, Russia;
Skobeltsyn Institute of Nuclear Physics, Moscow, Russia;
Petersburg Nuclear Physics Institute, Gatchina, Russia;
Vinča Institute of Nuclear Sciences, Serbia;
Pavol Jozef Šafárik University, Košice, Slovakia



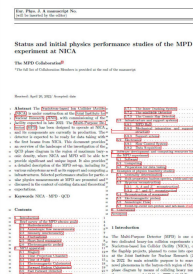
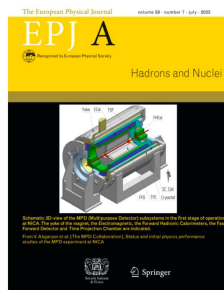
MPD publications, conferences and workshops

- International Workshop on physics performance studies at NICA
 - <http://indico.oris.mephi.ru/event/301>
 - 5 workshops since 2019



2nd China-Russia Joint Workshop on NICA Facility
indico.jinr.ru/event/4642

Over 50 reports at international conferences and workshops



Status and initial physics performance studies of the MPD, Eur.Phys.J.A 58 (2022) 7, 140

MPD Physics Program

G. Feofilov, P. Parfenov

Global observables

- Total event multiplicity
- Total event energy
- Centrality determination
- Total cross-section measurement
- Event plane measurement at all rapidities
- Spectator measurement

V. Kolesnikov, Xianglei Zhu

Spectra of light flavor and hypernuclei

- Light flavor spectra
- Hyperons and hypernuclei
- Total particle yields and yield ratios
- Kinematic and chemical properties of the event
- Mapping QCD Phase Diag.

K. Mikhailov, A. Taranenko

Correlations and Fluctuations

- Collective flow for hadrons
- Vorticity, Λ polarization
- E-by-E fluctuation of multiplicity, momentum and conserved quantities
- Femtoscopy
- Forward-Backward corr.
- Jet-like correlations

D. Peresunko, Chi Yang

Electromagnetic probes

- Electromagnetic calorimeter meas.
- Photons in ECAL and central barrel
- Low mass dilepton spectra in-medium modification of resonances and intermediate mass region

Wangmei Zha, A. Zinchenko

Heavy flavor

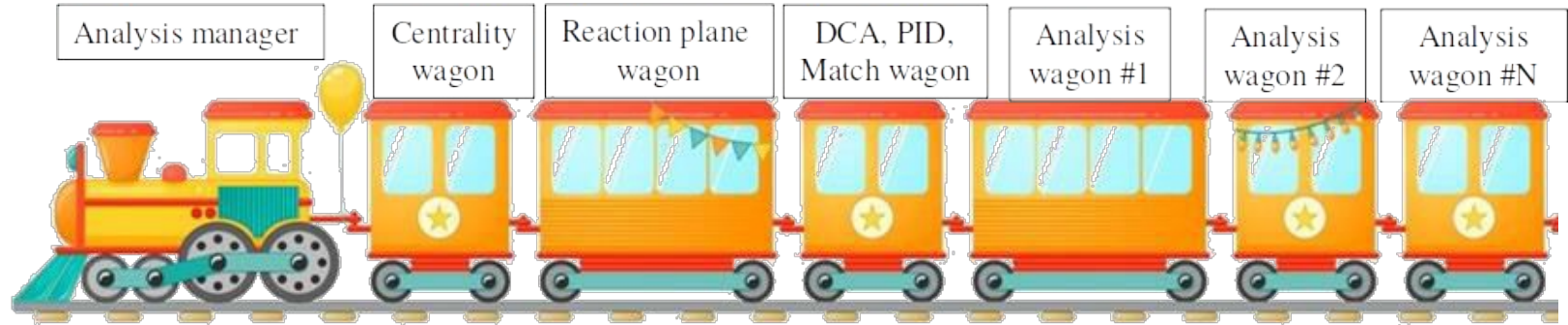
- Study of open charm production
- Charmonium with ECAL and central barrel
- Charmed meson through secondary vertices in ITS and HF electrons
- Explore production at charm threshold

Big Data Production

Physics feasibility studies using centralized large-scale MC productions \Rightarrow consistent picture of the MPD physics capabilities with the first data sets, preparation for real data analyses.

A new cycle of productions (<https://mpdforum.jinr.ru/c/mcprod/26>):

Centralized Analysis Framework for access and analysis of data \Rightarrow Analysis Train:



Regular runs on request since September, 2023 \Rightarrow ~12 hours to process 50M events for 10–15 wagons

Many new services and improvements (improved PID parametrizations, new wagons):

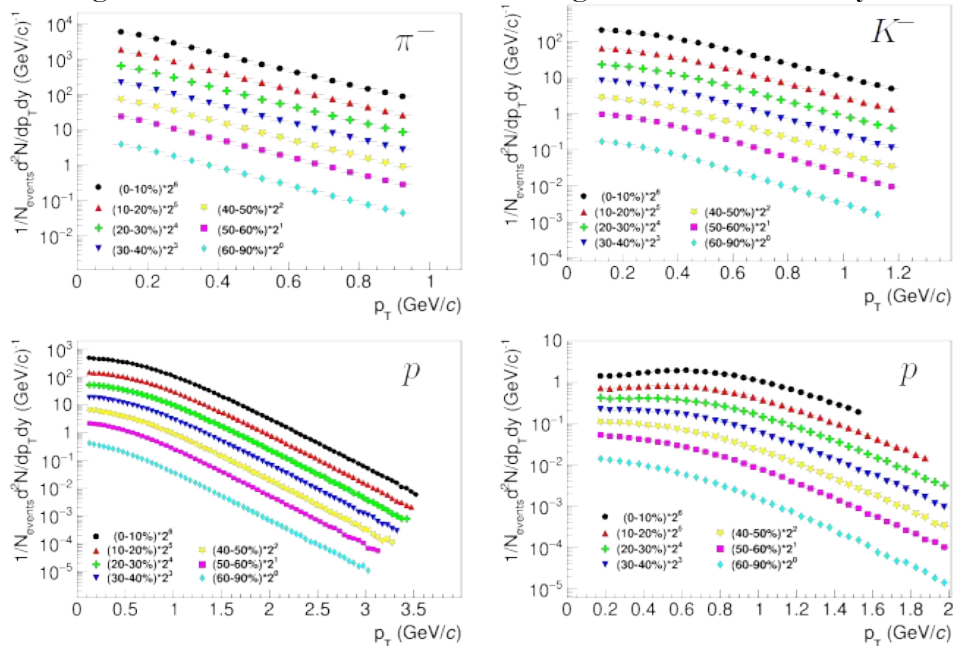
New standard for physics feasibility studies \Rightarrow ideally all analysis codes should be committed to MpdRoot as Wagons

Physics feasibilities studies

Identified charged hadrons ($\pi/K/p$)

BiBi@9.2 GeV (UrQMD), 50 M events \gg full event/detector reconstruction

$\pi/K/p$ identification based on n-sigma selections in the TPC/TOF \gg good for the first day measurements



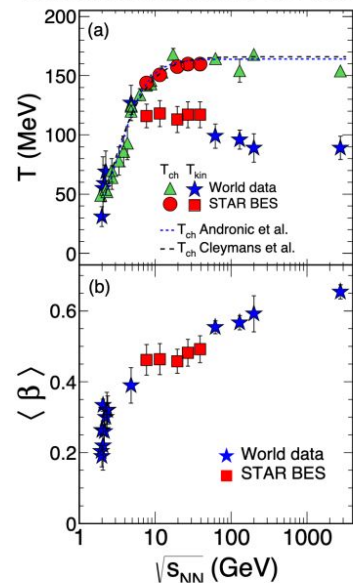
Good enough coverage for dN/dy , $\langle p_T \rangle$ and β/T (BW-fits) measurements.

Unmeasured low- p_T range is as small as possible with the existing track reconstruction methods

Sampled yields $> 92\%$ for all species

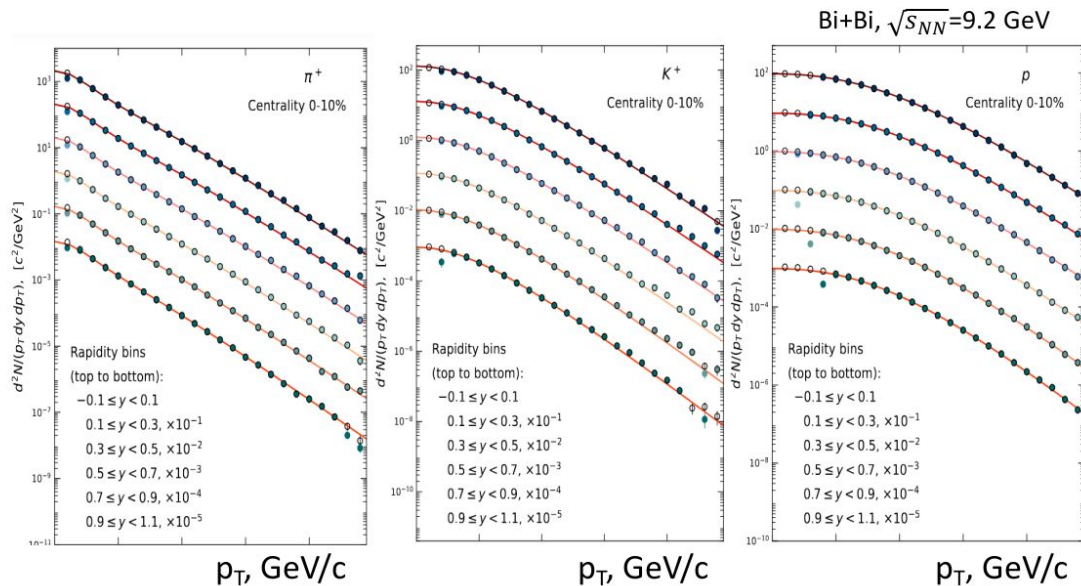
Identified charged hadrons

Phys.Rev.C 96 (2017) 4, 044904



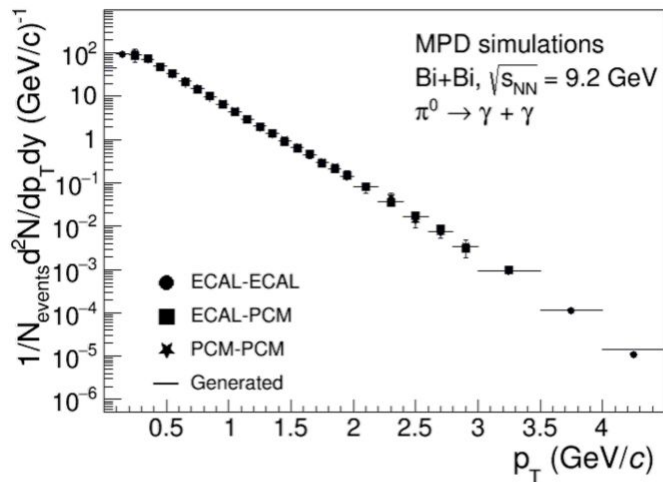
Particle yields allow to extract information about (μ_B, T_{ch})

Particle spectra allow to extract information about $(\langle \beta \rangle, T_{kin})$

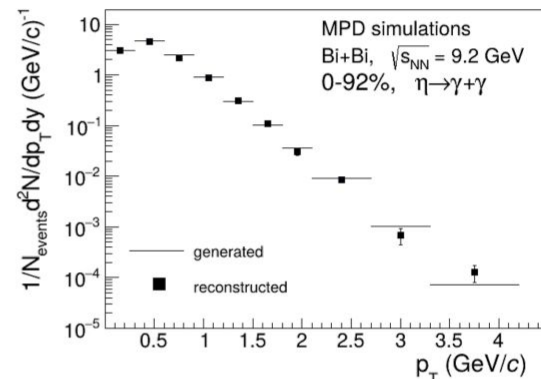
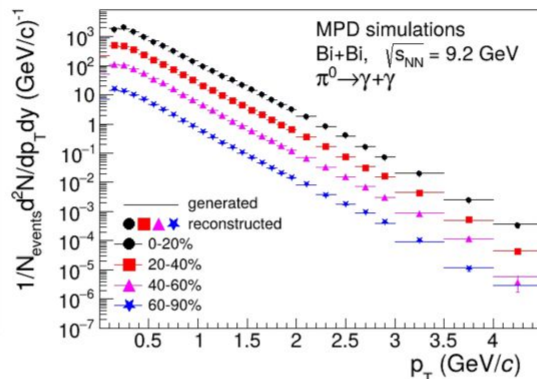


- Probe freeze-out conditions, collective expansion, mechanisms, strangeness production, parton energy loss, etc. with particles of different masses, quark contents/counts → **requirements on MPD acceptance and PID capabilities**
- Charged hadrons:** large ($\sim 70\%$ of $\pi/K/p$) and uniform acceptance + excellent PID capabilities of TPC and TOF from $p_T \sim 0.1$ GeV/c

Neutral identified hadron production

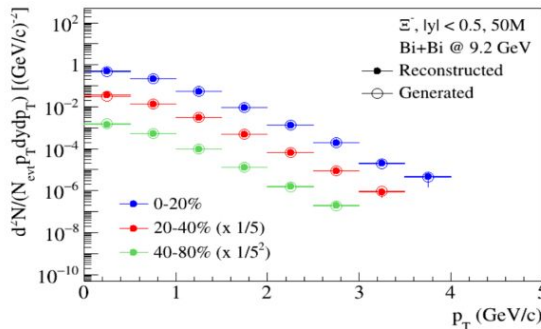
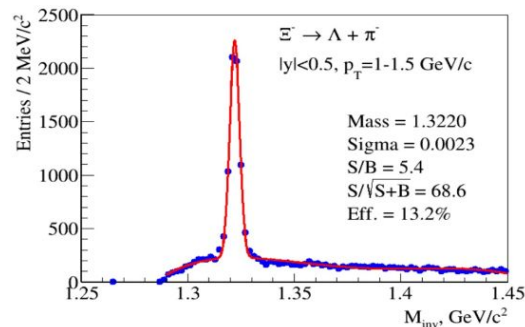
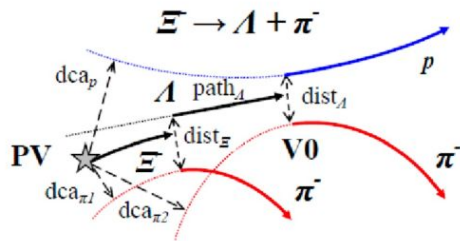
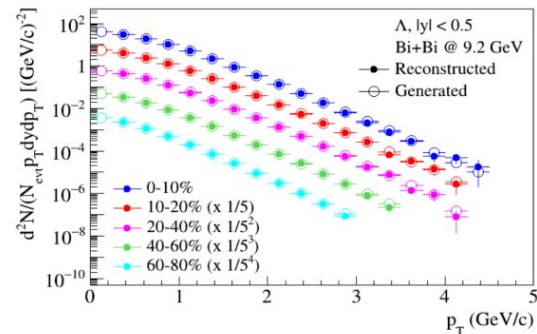
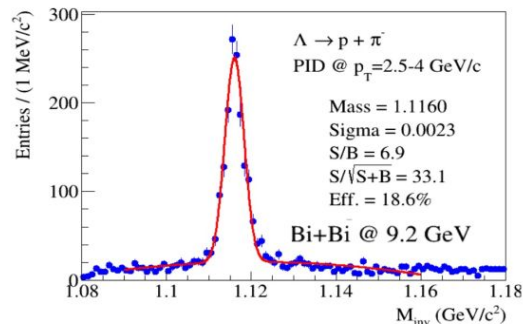
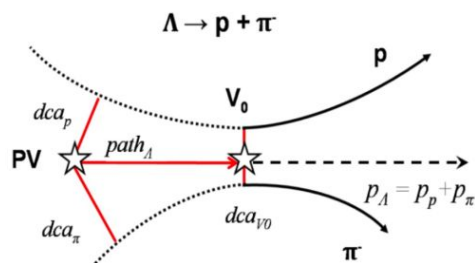


BiBi@9.2 GeV (UrQMD), 50 M events \rightarrow full event/detector reconstruction



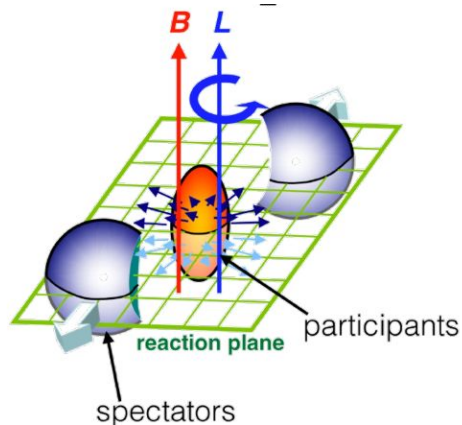
- MPD will be able to measure differential production spectra, integrated yields and $\langle p_T \rangle$, particle ratios, multiplicity distributions for a variety of identified hadrons ($\pi, K, \eta, \omega, \rho, \dots$)
- Neutral mesons ($\pi^0, K_S, \eta, \omega, \eta'$) : ECAL reconstruction + photon conversion method (PCM)
- Will be helpful to extend p_T ranges of charged particle measurements and assess systematics

Hyperon production



- Strangeness enhancement is considered to be a signature of the QGP formation with no consensus on the dominant mechanisms of strangeness enhancement – precise measurements are needed in pp, pA, AA
- Strange baryons can be reconstructed with a good level of significance (S/B ratios) with PID using TPC+TOF and different topology selections

Hyperon Global Polarization



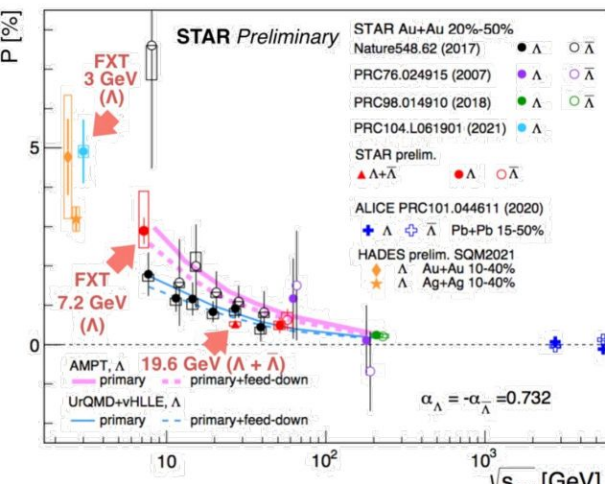
Can be defined as: $\frac{dN}{d\cos(\phi_\Lambda - \phi_p^*)} = \frac{1}{2}(1 + \alpha_\Lambda |P_\Lambda| \cos(\phi_\Lambda - \phi_p^*))$

Invariant mass fit method can be used to measure P_Λ :

$$P^{obs}(m_{inv}, p_T) = P^{sig}(p_T) \frac{N^{sig}(m_{inv}, p_T)}{N^{tot}(m_{inv}, p_T)} + P^{bg}(m_{inv}, p_T) \frac{N^{bg}(m_{inv}, p_T)}{N^{tot}(m_{inv}, p_T)}$$

$$\frac{8}{\pi \alpha_\Lambda R_{EP}} P^{sig}(p_T) = P_\Lambda + c \sin(\phi_\Lambda - \phi_p^*)$$

α_Λ - hyperon decay const., R_{EP} - EP resolution, ϕ_Λ, ϕ_p^* - azimuthal angles of Λ, p



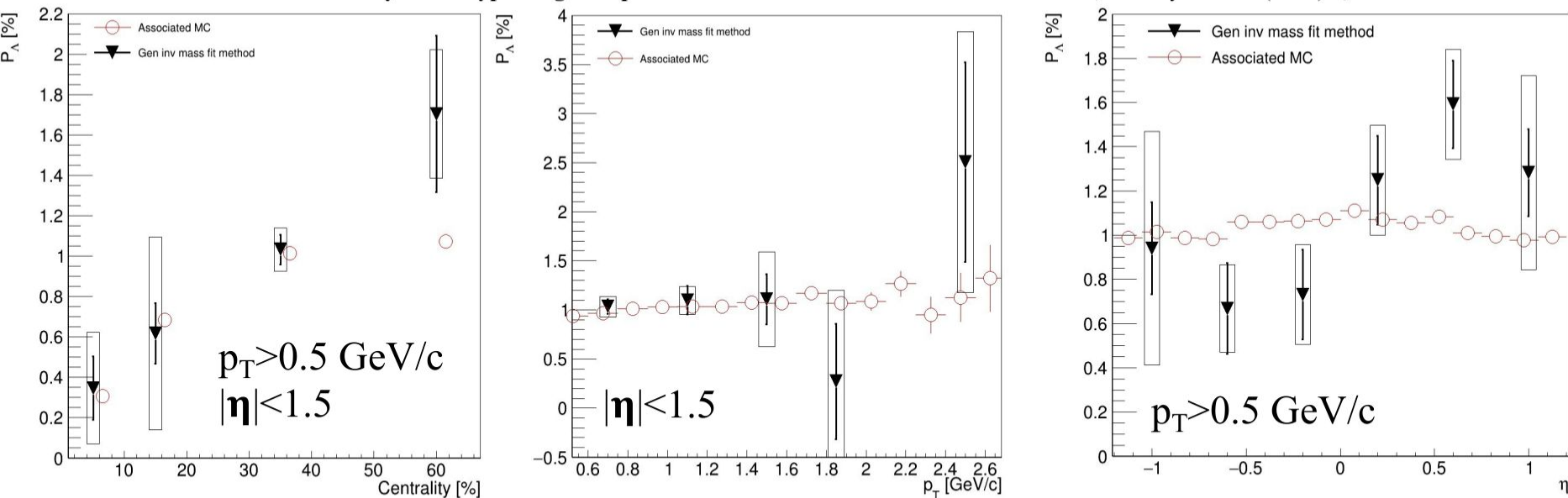
Focus is to see the effect of large angular momentum and magnetic field in heavy-ion collisions

- Global polarization of hyperons experimentally observed, decreases with $\sqrt{s_{NN}}$
 - reproduced by AMPT, 3FD, UrQMD+vHLL

P_Λ at NICA: extra points in the energy range 2-11 GeV centrality, p_T and rapidity dependence of polarization, not only for Λ , but other (anti)hyperons (Λ, Σ, Ξ)

Global Polarisation in MPD

Performance study of the hyperon global polarization measurements with MPD at NICA, Eur.Phys.J.A 60 (2024) 4, 85

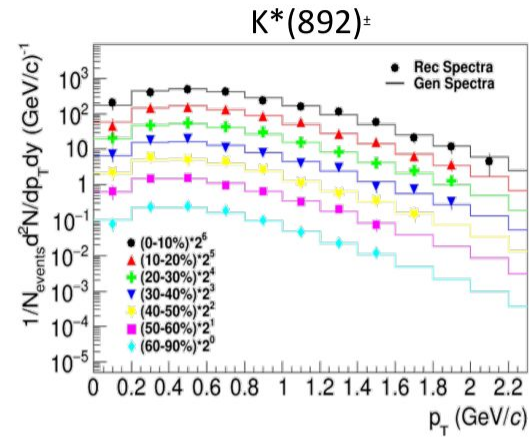
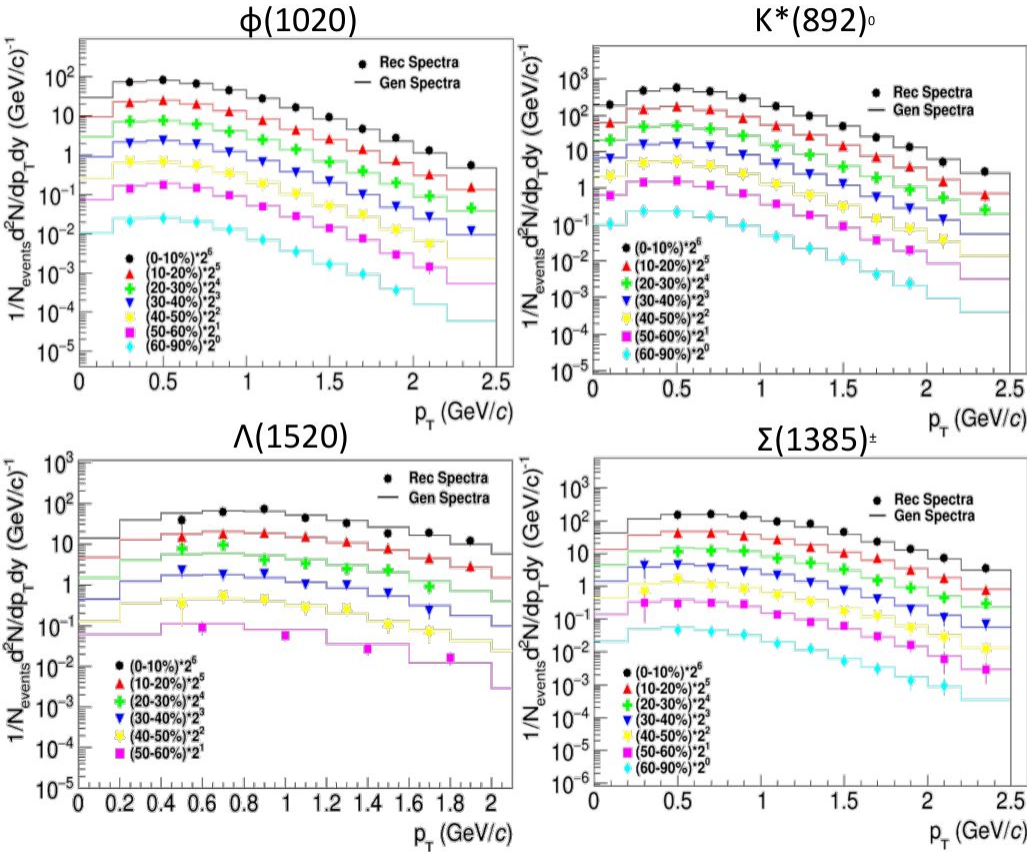


Good performance of MPD for P_Λ measurements

More statistics needed for differential (p_T, η) measurements and other hyperons

First results are to be expected at $\sim 100\text{M}$ events

Resonance production in MPD



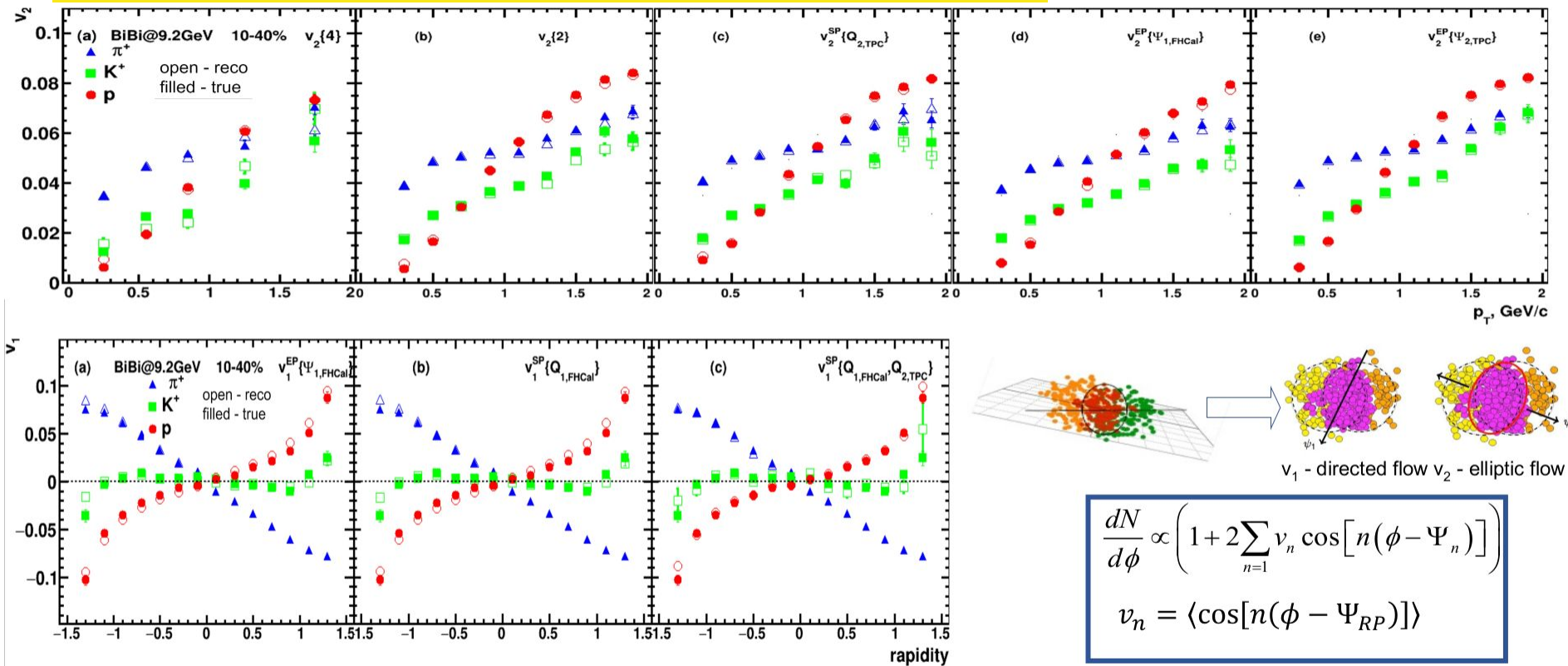
Short-lived resonances are sensitive to rescattering and regeneration in the hadronic phase

Most realistic approach to data analysis, centrality dependence

MPD is capable of resonance reconstruction using TPC and TOF for PID and selection based on the topology of the decay

First measurements are feasible with 10M events

Anisotropic flow of identified charged hadrons



Good performance for flow measurements for all methods used (EP, SP, Q-cumulants)

Anisotropic flow of V0 particles

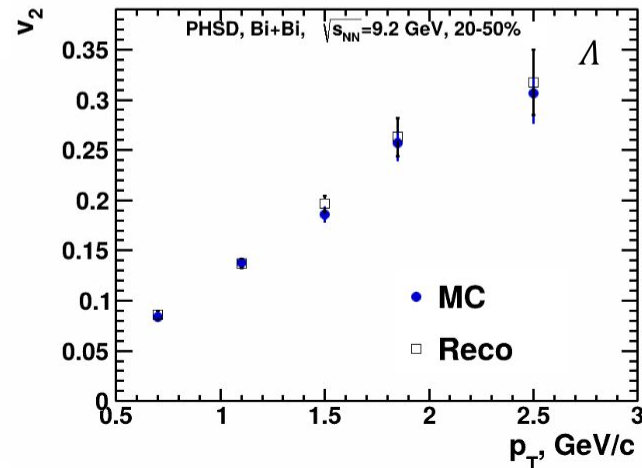
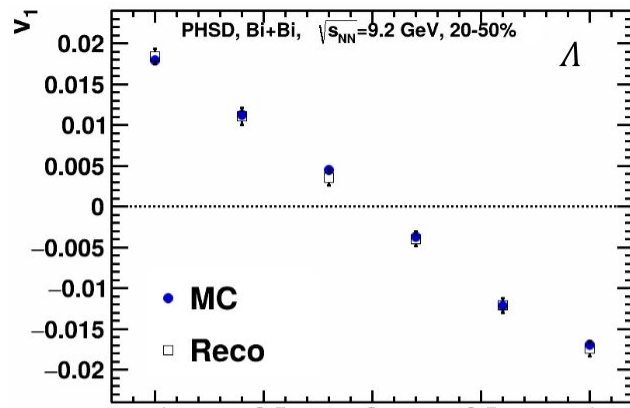
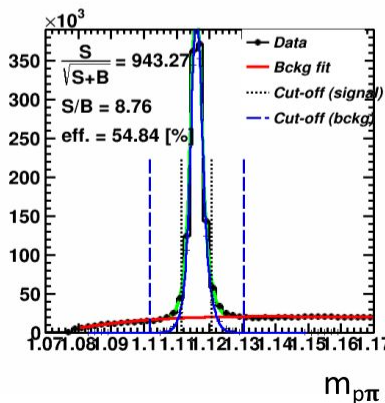
Differential flow can be defined using the following fit:

$$v_n^{SB}(\mathbf{m}_{inv}) = v_n^S \frac{N^S(\mathbf{m}_{inv})}{N^{SB}(\mathbf{m}_{inv})} + v_n^B(\mathbf{m}_{inv}) \frac{N^B(\mathbf{m}_{inv})}{N^{SB}(\mathbf{m}_{inv})}$$

where:

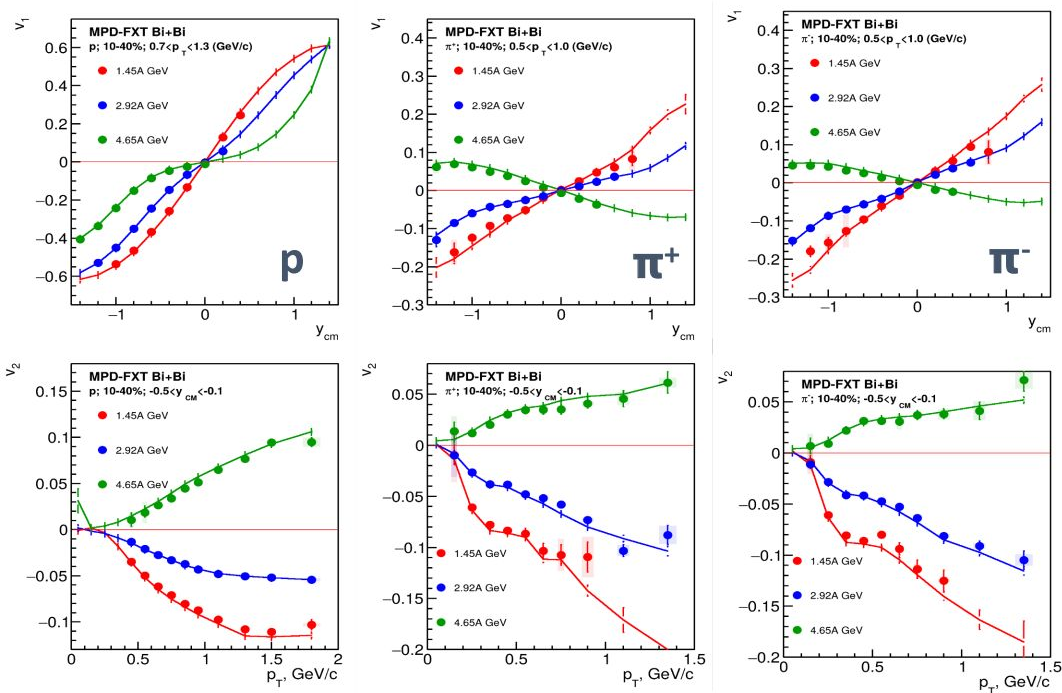
- v_n^S - signal anisotropic flow (set as a parameter in the fit)
- $v_n^B(\mathbf{m}_{inv})$ - background flow (set as polynomial function)
- $N^{SB}(\mathbf{m}_{inv})$ - \mathbf{m}_{inv} distribution (signal + background)
- $N^S(\mathbf{m}_{inv})$ - \mathbf{m}_{inv} signal distribution
- $N^B(\mathbf{m}_{inv})$ - \mathbf{m}_{inv} background distribution

Good performance for v_1 , v_2 using
invariant mass fit and event plane
methods

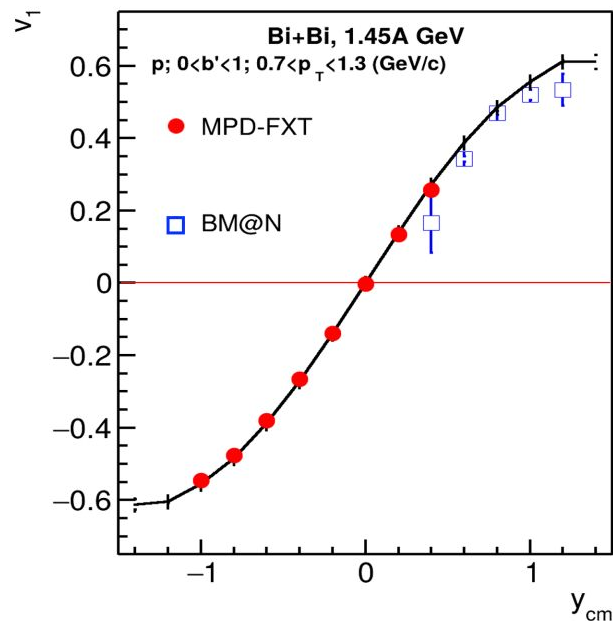


Anisotropic flow in MPD-FXT

- ❖ BiBi @ 2.5, 3.0 and 3.5 GeV (UrQMD mean-field, fixed-target mode)
- ❖ Realistic PID (TPC+TOF); efficiency corrections; centrality by TPC multiplicity



MPD vs. BM@N performance

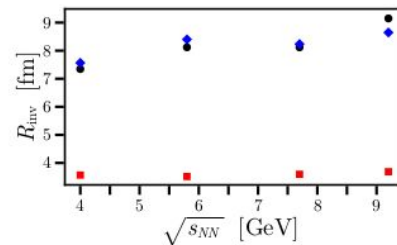
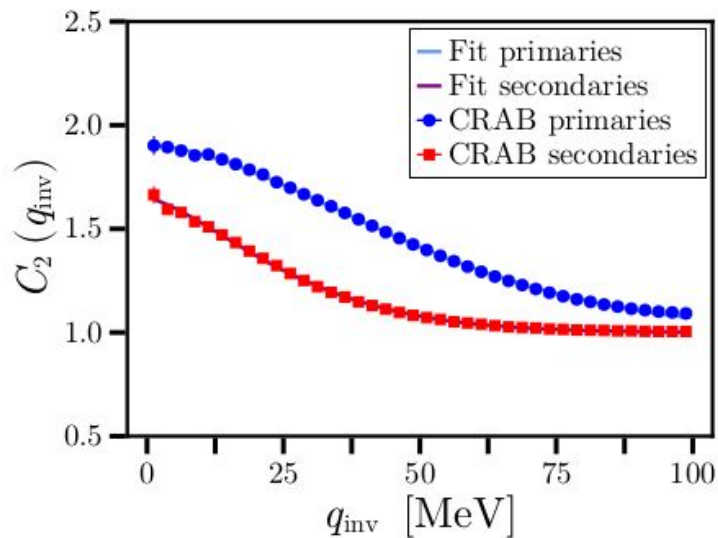


MPD and BM@N complete each other with a small overlap

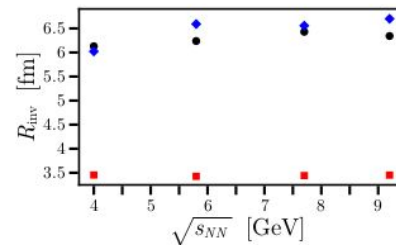
Measurement techniques were tested on experimental data from BM@N

Reconstructed v_1 & v_2 are quantitatively consistent with truly generated signals

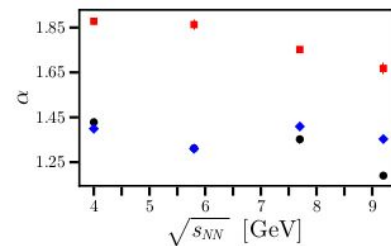
Two pion correlation function and Levy shape analysis



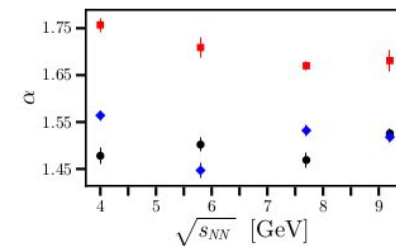
Ideal Resolution
 ● Complete set ● Primaries ● Secondaries



Finite Resolution
 ● Complete set ● Primaries ● Secondaries



Ideal Resolution
 ● Complete set ● Primaries ● Secondaries



Finite Resolution
 ● Complete set ● Primaries ● Secondaries

the core pion sample has a large component that comes from the decay of long-lived but slow moving resonances, as well as a small component of pions coming from primary processes

Summary



Preparation of the MPD detector and experimental program is continued

Start of the MPD commissioning in 2025 is the main goal

Develop physics program of the experiment, prepare tools and methods for data analysis

Thanks for your attention!